International Institute for Applied Systems Analysis
IIASA www.iiasa.ac.at

Single-gene speciation with pleiotropy: effects of allele dominance population size and delayed inheritance

Yamamichi, M. and Sasaki, A.

IIASA Interim Report
2013

International Institute for
Applied Systems Analysis
Schlossplatz 1
A-2361 Laxenburg, Austria

Tel: +43 2236 807 342
Fax: +43 2236 71313
E-mail: publications@iiasa.ac.at
Web: www.iiasa.ac.at

Interim Report **IR-13-075**

Single-gene speciation with pleiotropy: Effects of allele dominance population size and delayed inheritance

Masato Yamamichi
Akira Sasaki (sasaki@iiasa.ac.at)

Approved by

Ulf Dieckmann
Director, Evolution and Ecology Program

June 2015

Manuscript intended for Original Article of *Evolution*, December 4, 2012

Single-gene speciation with pleiotropy: Effects of allele dominance, population size, and delayed inheritance

Masato Yamamichi*[1], Akira Sasaki¶[2,3]

1) Department of Ecology and Evolutionary Biology, Cornell University, Ithaca, NY 14853, USA

2) Department of Evolutionary Studies of Biosystems, Graduate University for Advanced Studies (Sokendai), Hayama, Kanagawa, 240-0193, Japan

3) Evolution and Ecology Program, International Institute for Applied System Analysis, A-2361, Laxenburg, Austria

*corresponding author: my287@cornell.edu, Phone: +1-607-254-4231

¶: sasaki_akira@soken.ac.jp, Phone: +81-46-858-1537

Running Title: single-gene speciation with pleiotropy

Key Words: ecological speciation, magic trait, positive frequency-dependent selection, maternal effect, fixation probability, speciation gene

Figures 1, 2, 3, 4 (color), 5 (color), & 6; Table 1

Supporting information: 8 appendices with 1 supplement table & 6 supplement figures

No. of words in the main text: 5520

ABSTRACT

Single-gene speciation is considered to be unlikely, but an excellent example is found in land snails, in which a gene for left-right reversal has given rise to new species multiple times. This reversal might be facilitated by their small population sizes and maternal effect (i.e., 'delayed inheritance', in which an individual's phenotype is determined by the genotype of its mother). Recent evidence suggests that a pleiotropic effect of the speciation gene on anti-predator survival may also promote speciation. Here we theoretically demonstrate that, without a pleiotropic effect, in small populations the fixation probability of a recessive mutant is higher than a dominant mutant, but they are identical for large populations and sufficiently weak selection. With a pleiotropic effect that increases mutant viability, a *dominant* mutant has a higher fixation probability if the strength of viability selection is sufficiently greater than that of reproductive isolation, whereas a *recessive* mutant has a higher fixation probability otherwise. Delayed inheritance increases the fixation probability of a mutant if viability selection is weaker than reproductive isolation. Our results clarify the conflicting effects of viability selection and positive frequency-dependent selection due to reproductive isolation and provide a new perspective to single-gene speciation theory.

INTRODUCTION

Ever since Darwin, understanding the genetic and ecological conditions under which speciation occurs has been an ongoing challenge in evolutionary biology (Coyne and Orr 2004). One longstanding issue of debate in speciation theory concerns the number of genes that are necessary for speciation to occur. Under the classic Bateson-Dobzhansky-Muller (BDM) model, speciation requires changes in at least two genes because if there is one new allele with strong effects on heterozygote viability or mating compatibility but without epistasis to other genes, then the fitness of variants that harbor that allele should decrease, making the fixation of this allele in the population difficult. In contrast, negative epistatic interactions between independently derived alleles (A and B) at two loci can establish reproductive isolation between descendant genotypes (AAbb and aaBB) without reproductive isolation between the ancestral genotype (aabb) and daughter lineages (Bateson 1909; Dobzhansky 1936; Muller 1942).

Although the classical BDM incompatibility model has been influential in explaining the speciation process (Orr 1996; Gavrilets 2004; Bank et al. 2012), the model cannot explain the evolution of reproductive isolation via a single gene. Speciation that results from genetic substitution at a single locus is known as ‘single-gene speciation’ (Orr 1991).

Single-gene speciation has been of special interest for the following reasons: (1) “one-locus models are a natural starting point for theoretical approaches to many evolutionary phenomena” (Gavrilets 2004); (2) there are several examples of empirical evidence for the determination of mating traits by a single-locus (see Gavrilets 2004; Servedio et al. 2011 for review); and (3) a single speciation gene that pleiotropically contributes to reproductive isolation and divergent adaptation through a single trait ('automatic magic trait' according to Servedio et al. 2011) or several traits (Slatkin 1982) has been thought to promote ecological speciation (Rundle and Nosil 2005). Speciation becomes less probable if one locus is responsible for ecological adaptation and another locus is responsible for reproductive isolation because recombination breaks down the association between the two loci (Felsenstein 1981). Here, we refer to this dual function of a single gene as pleiotropic effects or simply pleiotropy (Slatkin 1982). In spite of these longstanding interests and an increasing number of studies that suggests the involvement of adaptation in speciation (Schluter 2009), the theoretical framework to explain the process of single-gene speciation is not robust because previous studies have relied heavily on numerical simulations (Kirkpatrick and Ravigné 2002; Gavrilets 2004). In this paper, we use new analytical results to investigate the effects of pleiotropy, allele dominance, population size, and maternal effect on the fixation

process of the speciation gene in single-gene speciation.

An excellent example of single-gene speciation is found in land snails (see Schilthuizen and Davison 2005; Okumura et al. 2008 for review). Handedness is shown to be controlled by two alleles at a single nuclear locus in phylogenetically segregated families of pulmonate snails (Boycott et al. 1930; Degner 1952; Murray and Clarke 1976; Freeman and Lundelius 1982; Ueshima and Asami 2003), and mating between opposite coiling individuals rarely occurs (Johnson 1982; Gittenberger 1988; Asami et al. 1998). Thus, the handedness gene is responsible for pre-mating isolation. Despite the positive frequency-dependent selection against rare mutants predicted by the BDM model (Johnson 1982; Asami et al. 1998), it has been shown that evolutionary transitions from an abundant dextral (clockwise coiling) species to a mutant sinistral (counter-clockwise coiling) species have occurred multiple times (Ueshima and Asami 2003; Davison et al. 2005; Hoso et al. 2010; Gittenberger et al. 2012).

Why is single-gene speciation possible in snails? Following Gittenberger (1988), Orr (1991) proposed that small population sizes and maternal effect (i.e., delayed inheritance: Fig. 1) in snail populations could promote single-gene speciation. Because snails have low mobility, local populations tend to be isolated from one another, which causes repeated

91 extinction and colonization events. Consequently, the effective population sizes of snails are
92 small and genetic drift is strong (Arnaud and Laval 2004; Hoso 2012). Delayed inheritance of
93 handedness is a type of maternal effect in which an individual's phenotype is determined by
94 the genotype of its mother (Fig. 1: Boycott et al. 1930; Degner 1952; Murray and Clarke
95 1976; Freeman and Lundelius 1982). Subsequent theoretical studies on the evolution of snail
96 coiling have basically attributed the cause of single-gene speciation to these two factors (van
97 Batenburg and Gittenberger 1996; Stone and Björklund 2002; but see Davison et al. 2005).
98 In a recent study (Hoso et al. 2010), a 'right-handed predator' hypothesis was
99 proposed to explain the effects of pleiotropy on the single-gene speciation of snails. The
100 authors concluded that a gene controlling coiling direction of snails could pleiotropically
101 affects interchiral mating difficulty and anti-predator adaptation because of the 'handedness'
102 of the predator. Because most snails are dextral ('right-handed') (Vermeij 1975), predators
103 tend to be 'right-handed' (have evolved to specialize in the abundant dextral type of snail).
104 Such predators include box crabs (Shoup 1968; Ng and Tan 1985; Dietl and Hendricks 2006),
105 water-scavenger beetle larvae (Inoda et al. 2003), and snail-eating snakes (Hoso et al. 2007;
106 Hoso et al. 2010). Behavioral experiments revealed that right-handed predators tend to fail in
107 attempts to eat sinistral snails because of the left-right asymmetry of their feeding apparatuses

and behaviors (Inoda et al. 2003; Dietl and Hendricks 2006; Hoso et al. 2007). Therefore, although a mating disadvantage still exists, sinistral snails will have a survival advantage under right-handed predation. This can potentially promote the fixation of a sinistral allele, and indeed Hoso et al. (2010) found a positive correlation between the distribution of a right-handed predator (snake) and proportion of sinistral lineages in Southeast Asia. Although Hoso et al. (2010) showed a correlation *pattern*, the fixation *process* of the mutant allele in the speciation gene with pleiotropic effects underlying such pattern has not been fully investigated.

Here, we theoretically investigate the fixation process of a mutant allele in the speciation gene in single-gene speciation with and without pleiotropic effects. We seek to answer the following questions. (1) How do allele dominance, population size, and delayed inheritance affect single-gene speciation? What kind of mutant allele dominance (e.g., dominant, recessive, or subdominant) has the highest fixation probability? How do population size and delayed inheritance affect this tendency? (2) How does pleiotropy affect the process of single-gene speciation? On the one hand, when the mutant frequency is low, it would be better for heterozygotes to have the resident phenotype to mate with common resident genotypes because of positive frequency-dependent selection. On the other hand, the mutant

phenotype is advantageous under strong viability selection. Because of the conflicting factors acting on heterozygotes, the overall effects of allele dominance and delayed inheritance can be changed by the relative strengths of the pleiotropic effects of the speciation gene.

MODEL

To examine the questions of single-gene speciation described above, we consider a general allopatric speciation model. When a panmictic population splits into two geographically divided subpopulations, it is sufficient to compare fixation probabilities of a mutant allele in a single subpopulation to understand the likelihood of speciation (Orr 1991). We construct Wright-Fisher models of haploid or diploid individuals without delayed inheritance and diploid individuals with delayed inheritance to study the mutant allele frequency change through generations with reproductive isolation and viability selection.

We assume that mating partners are randomly chosen from the population and that mating between different phenotypes fails with probability r (Table 1) because of either pre- or post-zygotic factors (Slatkin 1982). A common phenotype enjoys an advantage over a rare one because a randomly chosen mate is more likely to be compatible (i.e., the same phenotype). This leads to positive frequency-dependent selection (favoring the more common

142 phenotype) in the mating character.

143

144 **Haploid model**

145 We first consider the simplest case of haploid inheritance. We denote the frequency

146 of the mutant allele (A) by p and that of the wild type allele (a) by $1 - p$. The frequency after

147 mating, $\tilde{p}$, is

148

149 $$\tilde{p} = \frac{p^2 + (1-r)p(1-p)}{1-2rp(1-p)}, \quad (1)$$

150

151 where r measures the intensity of reproductive isolation between the mutant and wild type (0

152 $\leq r \leq 1$, Table 1). Reproductive isolation is complete if $r = 1$, the mating is random if $r = 0$,

153 and reproductive isolation is partial if $0 < r < 1$. The mutant frequency after one generation,

154 p', is given by

155

156 $$p' = \frac{(1+s)\tilde{p}}{(1+s)\tilde{p} + 1\cdot(1-\tilde{p})}, \quad (2)$$

157

158 where s is a positive viability selection coefficient for a mutant (i.e., a mutant has higher

159 survivorship than a wild type). For example, if a mutant snail is sinistral, s represents the
160 relative survival advantage of sinistral snails because of the right-handed predation by snakes
161 (Hoso et al. 2010).
162
163 **Diploid model without delayed inheritance**
164 For the diploid model without delayed inheritance, a mutant arises as a single
165 heterozygote (Aa) in a population of the wild type homozygotes (aa). We denote the degree of
166 dominance of allele A by h such that $h = 0$ and $h = 1$ correspond to completely recessive and
167 dominant mutant alleles, respectively. Under partial dominance ($0 < h < 1$), we consider two
168 models. First, a three-phenotype model in which heterozygotes have an intermediate
169 phenotype of the homozygous phenotypes, and the intensities of reproductive isolation and
170 viability selection are determined by the degree of dominance (h), although this does not
171 apply to snails (Table 1). Second, a two-phenotype (A and a) model in which a heterozygote
172 has phenotypes A and a with probabilities h and $1 – h$, respectively (Appendix S8). We adopt
173 the former model in the main text, but both models give qualitatively similar results (see
174 Discussion). The frequencies of genotypes AA ($= x$) and Aa ($= y$) after mating, $\tilde{x}$ and $\tilde{y}$, are
175 given by

176

$$T\tilde{x} = x^2 + \left[1-(1-h)r\right]xy + \frac{y^2}{4},$$
$$T\tilde{y} = \left[1-(1-h)r\right]xy + 2(1-r)xz + \frac{y^2}{2} + (1-hr)yz, \quad (3)$$

177

178

179 where $T = 1-2r\left[(1-h)xy + xz + hyz\right]$ and z (= 1 − x − y) represents the frequency of the

180 resident allele homozygote, aa (Table 1). The frequencies in the next generation, x' and y',

181 are

182

$$x' = \frac{(1+s)\tilde{x}}{(1+s)\tilde{x} + (1+hs)\tilde{y} + 1\cdot\tilde{z}},$$
$$y' = \frac{(1+hs)\tilde{y}}{(1+s)\tilde{x} + (1+hs)\tilde{y} + 1\cdot\tilde{z}}, \quad (4)$$

183

184

185 where s is the selective advantage of the mutant phenotype in terms of viability. By definition,

186 $\tilde{z} = 1-\tilde{x}-\tilde{y}$.

187 The condition for the invasion of the mutant allele in a population of infinite size is

188 analyzed by examining the local stability of equilibrium without the mutant (x = y = 0) in

189 equation (4). The fixation probability of a mutant for the case with random genetic drift

190 because of a finite population size is examined in three ways. First, assuming r and s values

191 are small, a two-dimensional representation of genotype dynamics (4) can be approximated
192 with one-dimensional dynamics along Hardy-Weinberg equilibrium (Fig. 2). Then applying
193 the diffusion approximation (Crow and Kimura 1970) leads to an analytical formula for the
194 fixation probability with an arbitrary degree of dominance for the mutant allele. Second, for a
195 very small population, because the diffusion approximation is not applicable, the exact
196 fixation probability is numerically calculated with a Markov chain approach (first-step
197 analysis, Pinsky and Karlin 2010). Third, the fixation probability is estimated from extensive
198 Monte Carlo simulations of full dynamics (4) under random genetic drift. We assume
199 symmetric mutation rates for the dominant and recessive alleles and compare their fixation
200 probabilities to predict the allele dominance of sinistral alleles in snails.
201
202 **Diploid model with delayed inheritance**
203 With delayed inheritance, the phenotype of an individual is determined by its
204 mother's genotype. In this model, 6 pairs of genotype-phenotype combination are possible;
205 however, with complete recessiveness or dominance, only 5 pairs can be realized. Here, we
206 assume that the mutant allele A is completely dominant. The counterpart case for a completely
207 recessive mutant can be analyzed in a parallel manner (see Appendix S2). With three

genotypes (AA, Aa, and aa) and two phenotypes (A and a), the six genotype-phenotype combinations are denoted as AA_A, AA_a, Aa_A, Aa_a, aa_A, and aa_a. For example, Aa_A represents an individual with genotype Aa and phenotype A. Because allele A is dominant, AA_a is simply impossible in the genetic system of delayed inheritance (Table S1).

We assume that the mutation in the speciation gene occurs in the embryo. In the genetic system of delayed inheritance, the first mutant's phenotype is the same as its wild type mother. We denote the frequencies of each combination of genotypes and phenotypes, AA_A, Aa_A, Aa_a, aa_A, and aa_a by x_A, y_A, y_a, z_A, and z_a (= $1 - x_A - y_a - z_A - z_a$), respectively. Let p (= $x_A + (y_A + y_a)/2$) and q (= $1 - p = (y_A + y_a)/2 + z_A + z_a$) be the frequencies of dominant (A) and recessive (a) alleles. The frequencies after mating are

$$
\begin{aligned}
T\tilde{x}_A &= p^2 - r y_a\left(x_A + \frac{y_A}{2}\right),\\
T\tilde{y}_A &= p(1-x_A) - r\left[z_a\left(x_A + \frac{y_A}{2}\right) + y_a\left(x_A + y_A + \frac{z_A}{2}\right)\right],\\
T\tilde{y}_a &= p(1+x_A-2p) - r\left[z_a\left(x_A + \frac{y_A}{2}\right) + \frac{y_a z_A}{2}\right],\\
T\tilde{z}_A &= (p-x_A)(1-p) - \frac{r}{2}\left[y_A(y_a+z_a) + y_a z_A\right],
\end{aligned}
\tag{5}
$$

where $T = 1 - 2r(x_A + y_A + z_A)(y_a + z_a)$. Because phenotype A is favored under viability selection, the frequencies after viability selection are given by

223

224 $$x'_{\mathrm{A}}=\frac{(1+s)\tilde{x}_{\mathrm{A}}}{W}, y'_{\mathrm{A}}=\frac{(1+s)\tilde{y}_{\mathrm{A}}}{W}, y'_{\mathrm{a}}=\frac{\tilde{y}_{\mathrm{a}}}{W}, z'_{\mathrm{A}}=\frac{(1+s)\tilde{z}_{\mathrm{A}}}{W}, z'_{\mathrm{a}}=\frac{\tilde{z}_{\mathrm{a}}}{W}, \quad (6)$$

225

226 where $W=1+s(\tilde{x}_{\mathrm{A}}+\tilde{y}_{\mathrm{A}}+\tilde{z}_{\mathrm{A}})$ is the mean fitness of the population. See Appendix S2 for the

227 case of a recessive mutant allele.

228 Similar to the without-delayed-inheritance model, the condition in which the mutant

229 invades a population of infinite size is analyzed by examining the local stability of

230 mutant-free equilibrium, $x_A=y_A=y_a=z_A=0$, with 4-dimensional genotype dynamics

231 (5)-(6). For the fixation probability of the mutant in a finite population, genotype dynamics

232 are reduced to a single dimension by assuming small *r* and *s*, through Hardy-Weinberg and

233 quasi-equilibrium of genotype-phenotype combination frequencies with the maternal

234 inheritance dynamics, which also leads to an analytical formulation. The first-step analysis for

235 a very small population and the Monte Carlo simulations are performed in the same manner

236 as in the case without delayed inheritance.

237 First-step analysis can also be applied to large populations, but the calculation is

238 formidable when *N* is large (especially for the diploid model with delayed inheritance that has

239 four variables). Therefore, we present results for the $N = 3$ condition and compare these

240 results to the $N = 10$, $N = 1{,}000$ (Monte Carlo simulations), and $N \to \infty$ (diffusion
241 approximation) conditions.
242
243 **RESULTS**
244 Through a deterministic analysis of infinite populations, we confirm that if the
245 degree of reproductive isolation between mating phenotypes is larger than the coefficient of
246 viability selection ($r > s$), the system shows bistability: the monomorphism of either allele (A
247 or a) is stably maintained under positive frequency-dependent selection due to reproductive
248 isolation for haploid and diploid conditions as well as delayed and non-delayed inheritance
249 conditions. A rare mutant allele cannot invade infinite populations as predicted by the classic
250 theory (Bateson 1909; Dobzhansky 1936; Muller 1942). Thus, genetic drift in finite
251 populations is a prerequisite for single-gene speciation with weak viability selection ($r > s$)
252 (Gavrilets 2004).
253
254 **Invasion conditions in deterministic models**
255 We demonstrate that pleiotropic effects can promote single-gene speciation, as
256 proposed by Hoso et al. (2010). Because a single speciation gene causes positive

257 frequency-dependent selection, viability selection must be strong enough for the mutant allele
258 to successfully invade a population (Fig. 3). The required selection coefficient for a mutant
259 allele to invade is $s > r/(1-r)$ in haploid and diploid models with complete dominance (i.e.,
260 the mutant is either completely dominant or recessive) and $s > r/(1-hr)$ for the diploid
261 model with partial dominance (Appendix S1, S2, and S8). In the haploid model, equations (1)
262 and (2) are approximated as $p' \approx (1+s)(1-r)p$ if the mutant frequency is small ($p \approx 0$).
263 When $(1 + s)(1 - r) < 1$, the system is bistable and positive frequency-dependent selection
264 excludes rare alleles. There are two locally stable equilibria at $p = 0$ and $p = 1$, and a locally
265 unstable equilibrium, $p_c = [r(1+s)-s]/[r(2+s)]$, that divides two basins of attraction. As
266 the mutant allele becomes more selectively favored (s (> 0) is increased), the unstable
267 equilibrium moves closer to zero and eventually disappears once s is large enough to satisfy
268 $(1 + s)(1 - r) = 1$. When $(1 + s)(1 - r) > 1$ or $s > r/(1 - r)$, there is a globally stable equilibrium
269 at $p = 1$ and the mutant allele increases and eventually fixes irrespective of its initial
270 frequency (Fig. 3). Note that invasion is impossible when reproductive isolation is complete
271 ($r = 1$), and this again suggests the importance of genetic drift in small populations.
272 For the diploid model, partial dominance makes single-gene speciation more
273 feasible because heterozygotes can simultaneously maintain their mating probability and

274 survival advantage. We derive the condition for the mutant allele to be able to invade the wild
275 type population as $s > r/(1 - hr)$ when $h \neq 0$ by analyzing recursion equations (3) and (4)
276 (Appendix S1). Interestingly, the invasion condition of the complete recessive ($h = 0$) allele (s
277 $> r/(1 - r)$) differs from $s > r$, that is the limit of $h \rightarrow 0$ for the invasion condition of the
278 partially dominant mutant (Appendix S1) because with small h in the partial dominance
279 model, there is a stable internal (coexisting) equilibrium, which does not exist for complete
280 recessiveness (Fig. S4). Heterozygotes with a completely recessive mutant allele are neutral
281 for viability selection, but the invasion condition is equivalent to the completely dominant (h
282 $= 1$) allele (Fig. 3). In addition, because of a locally stable equilibrium in which the mutant
283 allele coexists with the resident allele if r is large and h is small (Fig. S4), the invasibility of a
284 mutant (Fig. 3) does not necessarily imply its fixation in the population. For the diploid model
285 with delayed inheritance, the invasion condition in infinite populations is $(1 + s)(1 - r) > 1$
286 (Appendix S2), which is identical to the haploid and diploid models without delayed
287 inheritance (Fig. 3). However, the largest eigenvalue of the Jacobian matrix in the linearized
288 system is smaller than the dominant allele in the diploid model without delayed inheritance
289 (Appendix S2), which corresponds to the fact that delayed inheritance makes the invasion of a
290 mutant more feasible in a finite population, which we discuss later. Note that under positive

frequency-dependent selection, viability selection does not need to be constantly strong. Once the mutant allele frequency exceeds the unstable equilibrium, the mutant phenotype becomes advantageous in mating and strong viability selection is no longer necessary.

Fixation in a finite population with haploid inheritance

The change in allele frequency after one generation, $\Delta p = p' - p$, in the haploid model is

$$\Delta p = \frac{p(1-p)\left[r(2p-1)+s-sr(1-p)\right]}{(1+s\tilde{p})\left[1-2rp(1-p)\right]}, \tag{7}$$

which is derived from equations (1) and (2). Assuming r and s are small, we can consider a continuous time model for the change in allele frequency. Neglecting higher order terms for r and s, we have the deterministic dynamics,

$$\dot{p} = p(1-p)\left[r(2p-1)+s\right]. \tag{8}$$

Equation (8) has two stable equilibria at $p = 0$ and $p = 1$, and an internal unstable equilibrium

308 at $p = p_c = (1 - s/r)/2$ when $r > s$. However, if $s \geq r$, only $p = 1$ is locally stable. When s

309 = 0, the unstable equilibrium is at $p = 1/2$ and the derivative of allele frequency dynamics is

310 negative when p is smaller than 1/2 and positive when p is larger than 1/2 (solid gray line in

311 Fig. 4A). This result for the haploid model serves as the baseline when we discuss the effects

312 of dominance and delayed inheritance.

313 If the population is finite, a single mutant can go to fixation and replace the wild

314 type even when $r > s$. Assuming r and s are small and the population size (N) is large, we

315 obtain the fixation probability of a single mutant by applying the diffusion approximation as

316

317 $$\rho = u(1/N) = \frac{1/N}{\int_0^1 \exp\left[\frac{R}{2}\left(p - p^2\right) - \frac{S}{2}p\right]dp}, \quad (9)$$

318

319 where $R = 4Nr$ and $S = 4Ns$. If and only if the locally unstable equilibrium is less than 1/3,

320 $p_c = (1 - S/R)/2 < 1/3$, there exists some N with which the fixation probability ρ is higher

321 than that of a neutral mutant ($1/N$) (one-third law, Nowak et al. 2004).

322

Fixation in a finite population with diploid inheritance

The one-dimensional diffusion process along the curve of Hardy-Weinberg equilibrium

The dynamics of dominant and recessive alleles in the diploid models are also subject to positive frequency-dependent selection, but variation in the position of the internal equilibrium and selection gradient along the mutant allele frequency depends heavily on which allele is dominant, which has a large effect on the process of fixation. Namely, a dominant allele is favored over a recessive allele at intermediate frequencies; whereas, a recessive allele is favored when it is at either low or high frequencies (compare red and blue dashed curves in Fig. 4D). To show this and to evaluate the fixation probability of a mutant later, we approximate the two-dimensional genotype frequency dynamics of the diploid model to one-dimensional allele frequency dynamics. Genotype frequency dynamics are not strictly at Hardy-Weinberg (HW) equilibrium, and this deviation is caused by reproductive isolation and viability selection (Fig. 2). However, we show that if both r and s are small, frequency dynamics first approach HW equilibrium and slowly converge to a locally stable equilibrium at $p = 0$ or 1 (Crow and Kimura 1970 demonstrated this without viability selection). Assuming that r and s are in the order of ε, which is a small positive constant, we expand the dynamics of equations (3) and (4) in Taylor series with respect to ε. The leading order dynamics for the zygote frequencies becomes

$$x' = p^2 + O(\varepsilon),$$
$$y' = 2p(1-p) + O(\varepsilon). \tag{10}$$

Thus, up to the leading order, genotype frequencies are in HW equilibrium. From this, it follows that the allele frequencies do not change with time ($p' = p$) up to the leading order. By assuming a large population size, small values of r and s, and HW equilibrium (10), we can approximate the deterministic allele frequency dynamics by

$$\dot{p} = p(1-p)\left\{r\left[p(2p^2-1) - h(6p^2-6p+1)\right] + s\left[p + h(1-2p)\right]\right\}. \tag{11}$$

The scaled derivatives of the frequency dynamics when h = 0, 1/2, and 1 without viability selection (s = 0) are shown by dotted lines (Figs. 4 and S1).

Effect of dominance on the fixation probability of a mutant in a large finite population

Despite the large difference in the frequency-dependent fitness profiles between dominant and recessive alleles (Fig 4D), both alleles have the same fixation probability if there is no viability selection in large populations (Fig. 5H). From the allele frequency

dynamics (11) under Hardy-Weinberg equilibrium that is approximately followed throughout the process for small r and s, we obtain the fixation probability of a single mutant allele, $\rho_h = u(1/(2N))$, with the diffusion approximation (Appendix S3) where $u(p)$ is the fixation probability of a mutant with the initial frequency p. The fixation probability of a single mutant ρ_h for a given degree h of dominance is given by

$$\rho_h = \frac{1/(2N)}{\int_0^1 \exp\left\{Ry(1-y)\left[\frac{y}{2}(1+y)-h(2y-1)\right]-Sy\left[\frac{y}{2}+h(1-y)\right]\right\}dy}, \tag{12}$$

where $R = 4Nr$ and $S = 4Ns$, as defined before. Thus, the recessive ($h = 0$) and dominant ($h = 1$) mutants have exactly the same fixation probability if there is no viability selection ($s = 0$),

$$\rho_0 = \frac{1/(2N)}{\int_0^1 \exp\left[\frac{R}{2}(1-y)y^2(1+y)\right]dy} = \frac{1/(2N)}{\int_0^1 \exp\left[\frac{R}{2}y(1-y)^2(2-y)\right]dy} = \rho_1, \tag{13}$$

which can be shown by changing the variables in the integral (Appendix S3).

373 *Very small populations*

374 When population size is very small and viability selection is absent, the recessive
375 mutant allele has a higher fixation probability than the dominant allele. We show this result
376 with Monte Carlo simulations (Fig. 5E) and numerical calculations of exact fixation
377 probabilities using first-step analysis (Fig. 5B, Appendix S5, S6). The discrepancy between
378 the cases of large (diffusion approximation results) and small population sizes could be
379 because of the different contributions of absolute numbers of individuals to the frequency
380 dynamics. Although we assume that a mutant first arises as a single heterozygous individual
381 in the diploid model, the initial mutant frequency is higher in a small population. Thus, the
382 first heterozygous individual with a dominant mutant allele is more strongly selected against
383 than a recessive mutant allele in small populations (Fig. 4D).

384

385 *Effect of delayed inheritance*

386 As shown in equations (14) and (15) below, delayed inheritance halves the strength
387 of positive frequency-dependent selection (Fig. 4), which increases the fixation probability of
388 a mutant in large populations (Fig. 5I). Assuming HW equilibrium when r and s are small
389 (Appendix S4), the approximated frequency dynamics of the dominant mutant allele in the
390 diploid model with delayed inheritance is given by

391

392 $$\dot{p} = \frac{1}{2} p(1-p)^2 \left[-r(2p^2 - 4p + 1) + s \right]. \quad (14)$$

393

394 Furthermore, the frequency dynamics of the recessive mutant allele is

395

396 $$\dot{p} = \frac{1}{2} p^2 (1-p) \left[r(2p^2 - 1) + s \right]. \quad (15)$$

397

398 Comparing these equations to equation (11) with $h = 1$ and $h = 0$, we find that the right-hand
399 side of equations (14) and (15) are exactly one-half of the right-hand side of equation (11)
400 with $h = 1$ and $h = 0$, respectively (solid lines in Fig. 4). Therefore, regardless of whether the
401 mutant allele is dominant or recessive, the fixation probabilities for a mutant are higher when
402 delayed inheritance is present than when delayed inheritance is absent (Fig. 5I, Appendix S4).
403 The fact that the magnitudes of r and s relative to the strength of genetic drift $1/N$ are halved
404 may be reinterpreted to mean that delayed inheritance effectively halves the effective
405 population size. This is probably because the phenotype is determined only by the mother's
406 genotype with no contribution from the father. The tendency for the model with delayed
407 inheritance to have higher fixation probabilities remains the same in small populations where

408 diffusion approximation cannot apply (Figs. 5C, 5F, Appendix S7). With delayed inheritance,
409 fixation probabilities can be increasing functions of reproductive isolation (r) when viability
410 selection is strong ($s >> 1$) and the population size is very small ($N = 3$), which contrasts the
411 general tendency (i.e., for fixation probabilities to be decreasing functions of reproductive
412 isolation) (Fig. S6).
413
414 *Effect of reproductive isolation and viability selection*
415 Positive frequency-dependent selection and viability selection work on the mutant
416 phenotype; therefore, individuals with the mutant phenotype get conflicting effects from the
417 two selection pressures when the mutant allele frequency is low. When reproductive isolation
418 is relatively weak, the survival advantage of the mutant phenotype exceeds its mating
419 disadvantage; on the other hand, with relatively strong reproductive isolation, the survival
420 advantage of the mutant phenotype cannot compensate for its mating disadvantage when the
421 mutant is rare. In large populations, the dominant and recessive mutant alleles have the same
422 fixation probability without pleiotropy (when $s = 0$: Fig. 5), whereas the dominant mutant
423 allele has higher fixation probability when $r = 0$ (Haldane's sieve: see Discussion). Thus
424 fixation probabilities of the dominant mutant allele are always higher than those of the

recessive allele. Delayed inheritance halves selection pressures (equations 14 and 15); this is advantageous when positive frequency-dependent selection due to reproductive isolation is strong (Fig. 4), but is not advantageous when viability selection is strong. Therefore, the dominant mutant allele without delayed inheritance has the highest fixation probability when reproductive isolation (Nr) is weak and viability selection (Ns) is strong, whereas the dominant mutant allele with delayed inheritance has the highest fixation probability when reproductive isolation is strong and viability selection is weak in large populations (Fig. 6C). In small populations, the recessive mutant allele with delayed inheritance has the highest fixation probability when reproductive isolation is strong and viability selection is weak (Figs. 6A, 6B). Therefore, the more frequently fixed allele can be dominant when viability selection is relatively strong (Fig. 6), which is in contrast to speciation without pleiotropy.

DISCUSSION

In finite populations without pleiotropy, dominant and recessive alleles have the same fixation probability in large populations; however, a recessive allele has a higher fixation probability in very small populations. The effects of population size are contrasting, but most left-right reversals are likely to have occurred in small isolated populations (Orr

1991; Hoso 2012). Therefore, the recessive mutant allele will fix more frequently than the dominant allele in the absence of right-handed predation, if the dominant and recessive mutations arise in the same probability.

There are conflicting arguments about allele dominance; Orr (1991) wrote "the probability of fixation of a maternal mutation is roughly independent of its dominance" in dioecious populations, whereas hermaphroditic populations with selfing "…*decrease* the chance that a dominant mutation will be fixed." In contrast, van Batenburg and Gittenberger (1996) showed that the dominant mutant allele has a higher fixation probability. We point out that this discrepancy is mainly because of different assumptions of the initial numbers of the mutant allele. Both Orr (1991) and we computed the fixation probability of a single mutant, whereas van Batenburg and Gittenberger (1996) even considered 16 invaders with the total population size 32, assuming mass invasion from neighboring sinistral populations. By accounting for the assumptions of each argument, the conflicting results can be explained because the recessive mutant allele has a higher fitness when it is rare, whereas the dominant mutant allele has a higher derivative when the frequency is intermediate (Fig. 4D). We changed the initial numbers of mutants in Monte Carlo simulations and obtained results to support this claim (data not shown). The fixation probability is usually calculated for a single

459 *de novo* mutation. Thus, as long as the initial mutant is a single heterozygote, we analytically
460 and numerically showed that the recessive mutant allele has a higher fixation probability in
461 small populations and both alleles have the same probability in large populations (Fig. 5).

462 The effect of reproductive isolation and viability selection (Fig. 6) is consistent with
463 "Haldane's sieve", where there is a bias against the establishment of recessive adaptive alleles
464 (Haldane 1924, 1927; Turner 1981). Previous studies revealed that certain factors, including
465 self-fertilization (Charlesworth 1992), adaptation from standing genetic variation (Orr and
466 Betancourt 2001), and spatial structure (Whitlock 2003), can change the fixation bias of allele
467 dominance. Our results showed that the adaptive mutation that pleiotropically contributes to
468 reproductive isolation can also change this bias.

469 We consider two cases of partial dominance ($h = 0.5$) in the diploid model without
470 delayed inheritance. Although these do not apply to snails, the results would be important for
471 understanding general single-gene speciation processes. Because of different fitness gradients
472 along allele frequencies (Fig. S1), the three-phenotype model has a higher fixation probability
473 than the two-phenotype model, which has similar results as the haploid model (Figs. 5B, 5E,
474 5H, S2, and S3). With pleiotropy, the fixation probability in the three-phenotype model is the
475 highest when reproductive isolation is strong and viability selection is weak in large

476 populations (Fig. S5C), while it is the highest in intermediate intensity of reproductive
477 isolation and viability selection in small populations (Figs. S5A and S5B).

478 In single-gene speciation in snails, the intensity of interchiral mating difficulty, r,
479 should be an important parameter; interchiral mating is almost impossible in flat-shelled
480 snails that perform two-way face-to-face copulation (large r), whereas it is relatively easy for
481 tall-shelled snails that can copulate by shell mounting (small r) (Asami et al. 1998). Therefore,
482 even with the same population size and right-handed predation pressure, the frequently fixed
483 allele dominance can be changed (Fig. 6A). When right-handed predation is weak or absent
484 and interchiral mating is difficult (flat-shelled snails), the frequently fixed allele should be
485 recessive. On the other hand, the frequently fixed allele can be dominant when right-handed
486 predation is strong and interchiral mating is easy (tall-shelled snails).

487 We have calculated fixation probabilities for various values of N, r, s, and the
488 dominance of the mutant allele. Phylogenetic information (Ueshima and Asami 2003; Hoso et
489 al. 2010) can be used to infer these parameters because the number of left-right reversals in
490 the phylogeny is influenced by fixation probabilities. Let P_S be the duration that the snail
491 phenotype remains sinistral, and P_D be the duration for dextrality. The expected sojourn time
492 in the sinistral phenotype is $P_S = 1/(N\mu\rho_D)$, where μ is the mutation rate of the speciation gene

493 changing to the dextral allele and ρ_D is the fixation probability of the mutant dextral allele.
494 Assuming that the mutation is symmetrical and population size is constant, the ratio of these
495 values is given by $P_S/P_D = (N\mu\rho_D)/(N\mu\rho_S) = \rho_D/\rho_S$. If left-right reversals have occurred
496 frequently, the ratio estimated from the phylogeny data should approach the theoretical
497 prediction. The extent of assortative mating, *r*, (Asami et al. 1998) and biased predation
498 pressure by right-handed predators, *s*, (Hoso et al. 2007; Hoso et al. 2010) are known from
499 experiments. Thus, it would be possible to estimate the population size and allele dominance
500 by statistical inference. However, in addition to the somewhat arbitrary assumptions of
501 constant population size, symmetrical mutation, and equilibrium states, reconstruction of
502 ancestral states is generally challenging when the trait evolves adaptively (Cunningham 1999).
503 Furthermore, we did not consider gene flow between spatially neighboring dextral and
504 sinistral populations (Davison et al. 2005) or internal selection against left-right reversal
505 (Utsuno et al. 2011). Thus, we propose these estimations as a future research subject.

506 In conclusion, although the conventional theory by Bateson, Dobzhansky and
507 Muller is still valid, our study has shown that single-gene speciation is likely to be more
508 realizable than previous studies have assumed by combining various factors including
509 recessiveness, delayed inheritance, small population size, and pleiotropic effects that increase

510 mutant viability. Specifically, delayed inheritance and pleiotropic effects of the speciation
511 gene (e.g., right-handed predation on snails) can promote single-gene speciation, which
512 supports the hypothesis that right-handed predation by specialist snakes is responsible for
513 frequent left-right reversals of land snails in Southeast Asia (Hoso et al. 2010). Sinistral
514 species have frequently evolved outside the snake range without right-handed predation, and
515 in this case, our study suggests that allele dominance is important as well as small population
516 size and delayed inheritance (Orr 1991). Interestingly, population size and pleiotropy can
517 change the effects of allele dominance and delayed inheritance on speciation. Ueshima and
518 Asami (2003) constructed a molecular phylogeny and speculated that the dextral allele
519 appears to be dominant for *Euhadra* snails based on the breeding experiments with a
520 *Bradybaena* species, citing van Batenburg and Gittenberger (1996); however, caution is
521 needed because reversal could occur by a *de novo* mutation and viability selection by
522 right-handed predators might be involved in speciation (Hoso et al. 2010). Recent
523 technological developments in molecular biology make it possible to investigate the
524 dominance of alleles in ecologically important traits as well as their ecological and
525 evolutionary effects (e.g., Rosenblum et al. 2010). Although the search for a coiling gene (the
526 speciation gene) in snails is still underway (e.g., Grande and Patel 2009; Kuroda et al. 2009),

our prediction—that the recessive allele has a higher fixation probability in the absence of specialist predators ($s = 0$) for flat-shelled snails (large r), whereas the dominant allele can have a higher fixation probability in the presence of specialist predators ($s > 0$) for tall-shelled snails (small r) —will be testable. This hypothesis could be tested, for example, by analyzing the correlations between the presence of right-handed predators and sinistral allele dominance.

ACKNOWLEDGEMENTS

We thank Dr. Masaki Hoso for discussion and valuable comments on our earlier manuscript. We also thank two anonymous reviewers, Prof. Stephen P. Ellner, Prof. Hisashi Ohtsuki, Whit Hairston, Joseph L. Simonis, and members of the Sasaki-Ohtsuki lab, the Hairston lab, and the Ellner lab for their helpful comments. M. Y. was supported by a Research Fellowship of the Japan Society for the Promotion of Science (JSPS) for Young Scientist (21-7611) and is supported by JSPS Postdoctoral Fellowship for Research Abroad (24-869). A. S. is supported by MEXT/JSPS KAKENHI, and the Graduate University for Advanced Studies (Sokendai).

LITERATURE CITED

Arnaud, J. F., and G. Laval. 2004. Stability of genetic structure and effective population size

545 inferred from temporal changes of microsatellite DNA polymorphisms in the land
546 snail *Helix aspersa* (Gastropoda: Helicidae). Biological Journal of the Linnean Society
547 82:89-102.
548 Asami, T., R. H. Cowie, and K. Ohbayashi. 1998. Evolution of mirror images by sexually
549 asymmetric mating behavior in hermaphroditic snails. American Naturalist
550 152:225-236.
551 Bank, C., R. Bürger, and J. Hermisson. 2012. The limits to parapatric speciation:
552 Dobzhansky-Muller incompatibilities in a continent-island model. Genetics
553 191:845-863.
554 Bateson, W. 1909. Heredity and variation in modern lights. Pp. 85-101 *in* A. C. Seward, ed.
555 Darwin and Modern Science. Cambridge University Press, Cambridge.
556 Boycott, A. E., C. Diver, S. L. Garstang, and F. M. Turner. 1930. The inheritance of
557 sinistrality in *Limnaea peregra* (Mollusca, Pulmonata). Philosophical Transactions of
558 the Royal Society B 219:51-131.
559 Charlesworth, B. 1992. Evolutionary rates in partially self-fertilizing species. American
560 Naturalist 140:126-148.
561 Coyne, J. A., and H. A. Orr. 2004. Speciation. Sinauer Associates, Inc., Sunderland.
562 Crow, J. F., and M. Kimura. 1970. An Introduction to Population Genetics Theory. Harper &
563 Row, Publishers, Inc., New York.
564 Cunningham, C. W. 1999. Some limitations of ancestral character-state reconstruction when
565 testing evolutionary hypotheses. Syst. Biol. 48:665-674.
566 Davison, A., S. Chiba, N. H. Barton, and B. Clarke. 2005. Speciation and gene flow between
567 snails of opposite chirality. PLoS Biology 3:e282.
568 Degner, E. 1952. Der erbgang der inversion bei *Laciniaria biplicata* MTG. Mitteilungen der
569 Hamburg Zoologisches Museum und Institut 51:3-61.
570 Dietl, G. P., and J. R. Hendricks. 2006. Crab scars reveal survival advantage of left-handed
571 snails. Biology Letters 2:439-442.
572 Dobzhansky, T. 1936. Studies on hybrid sterility. II. Localization of sterility factors in
573 *Drosophila pseudoobscura* hybrids. Genetics 21:113-135.
574 Felsenstein, J. 1981. Skepticism towards Santa Rosalia, or why are there so few kinds of
575 animals? Evolution 35:124-138.
576 Freeman, G., and J. W. Lundelius. 1982. The developmental genetics of dextrality and
577 sinistrality in the gastropod *Lymnaea peregra*. Wilhelm Roux's Archives of
578 Developmental Biology 191:69-83.
579 Gavrilets, S. 2004. Fitness Landscapes and the Origin of Species. Princeton University Press,

580 Princeton.
581 Gittenberger, E. 1988. Sympatric speciation in snails: a largely neglected model. Evolution
582 42:826-828.
583 Gittenberger, E., T. D. Hamann, and T. Asami. 2012. Chiral speciation in terrestrial pulmonate
584 snails. PLoS ONE 7:e34005.
585 Grande, C., and N. H. Patel. 2009. Nodal signalling is involved in left-right asymmetry in
586 snails. Nature 457:1007-1011.
587 Haldane, J. B. S. 1924. A mathematical theory of natural and artificial selection, Part I.
588 Transactions of the Cambridge Philosophical Society 23:19-41.
589 Haldane, J. B. S. 1927. A mathematical theory of natural and artificial selection, Part V:
590 selection and mutation. Proc. Camb. Philos. Soc. 28:838-844.
591 Hoso, M. 2012. Non-adaptive speciation of snails by left-right reversal is facilitated on
592 oceanic islands. Contributions to Zoology 81:79-85.
593 Hoso, M., T. Asami, and M. Hori. 2007. Right-handed snakes: convergent evolution of
594 asymmetry for functional specialization. Biology Letters 3:169-172.
595 Hoso, M., Y. Kameda, S. P. Wu, T. Asami, M. Kato, and M. Hori. 2010. A speciation gene for
596 left-right reversal in snails results in anti-predator adaptation. Nature Communications
597 1:133.
598 Inoda, T., Y. Hirata, and S. Kamimura. 2003. Asymmetric mandibles of water-scavenger
599 larvae improve feeding effectiveness on right-handed snails. American Naturalist
600 162:811-814.
601 Johnson, M. S. 1982. Polymorphism for direction of coil in *Partula suturalis*: behavioural
602 isolation and positive frequency dependent selection. Heredity 49:145-151.
603 Kirkpatrick, M., and V. Ravigné. 2002. Speciation by natural and sexual selection: Models
604 and experiments. American Naturalist 159:S22-S35.
605 Kuroda, R., B. Endo, M. Abe, and M. Shimizu. 2009. Chiral blastomere arrangement dictates
606 zygotic left-right asymmetry pathway in snails. Nature 462:790-794.
607 Muller, H. J. 1942. Isolating mechanisms, evolution, and temperature. Biological Symposia
608 6:71-125.
609 Murray, J., and B. Clarke. 1976. Supergenes in polymorphic land snails II. *Partula suturalis*.
610 Heredity 37:271-282.
611 Ng, P. K. L., and L. W. H. Tan. 1985. 'Right handedness' in heterochelous calappoid and
612 xanthoid crabs: suggestion for a functional advantage. Crustaceana 49:98-100.
613 Nowak, M. A., A. Sasaki, C. Taylor, and D. Fudenberg. 2004. Emergence of cooperation and
614 evolutionary stability in finite populations. Nature 428:646-650.

615 Okumura, T., H. Utsuno, J. Kuroda, E. Gittenberger, T. Asami, and K. Matsuno. 2008. The
616 development and evolution of left-right asymmetry in invertebrates: lessons from
617 *Drosophila* and snails. Developmental Dynamics 237:3497-3515.
618 Orr, H. A. 1991. Is single-gene speciation possible? Evolution 45:764-769.
619 Orr, H. A. 1996. Dobzhansky, Bateson, and the genetics of speciation. Genetics
620 144:1331-1335.
621 Orr, H. A., and A. J. Betancourt. 2001. Haldane's sieve and adaptation from the standing
622 genetic variation. Genetics 157:875-884.
623 Pinsky, M. A., and S. Karlin. 2010. An Introduction to Stochastic Modeling. Academic Press,
624 Burlington.
625 Rosenblum, E. B., H. Römpler, T. Schöneberg, and H. E. Hoekstra. 2010. Molecular and
626 functional basis of phenotypic convergence in white lizards at White Sands. Proc. Natl.
627 Acad. Sci. U. S. A. 107:2113-2117.
628 Rundle, H. D., and P. Nosil. 2005. Ecological speciation. Ecology Letters 8:336-352.
629 Schilthuizen, M., and A. Davison. 2005. The convoluted evolution of snail chirality.
630 Naturwissenschaften 92:504-515.
631 Schluter, D. 2009. Evidence for ecological speciation and its alternative. Science
632 323:737-741.
633 Servedio, M. R., G. S. Van Doorn, M. Kopp, A. M. Frame, and P. Nosil. 2011. Magic traits in
634 speciation: 'magic' but not rare? Trends in Ecology & Evolution 26:389-397.
635 Shoup, J. B. 1968. Shell opening by crabs of genus *Calappa*. Science 160:887-888.
636 Slatkin, M. 1982. Pleiotropy and parapatric speciation. Evolution 36:263-270.
637 Stone, J., and M. Björklund. 2002. Delayed prezygotic isolating mechanisms: evolution with
638 a twist. Proceedings of the Royal Society of London Series B-Biological Sciences
639 269:861-865.
640 Turner, J. R. G. 1981. Adaptation and evolution in *Heliconius*: A defense of neoDarwinism.
641 Annu. Rev. Ecol. Syst. 12:99-121.
642 Ueshima, R., and T. Asami. 2003. Single-gene speciation by left-right reversal - A land-snail
643 species of polyphyletic origin results from chirality constraints on mating. Nature
644 425:679.
645 Utsuno, H., T. Asami, T. J. M. Van Dooren, and E. Gittenberger. 2011. Internal selection
646 against the evolution of left-right reversal. Evolution 65:2399-2411.
647 van Batenburg, F. H. D., and E. Gittenberger. 1996. Ease of fixation of a change in coiling:
648 Computer experiments on chirality in snails. Heredity 76:278-286.
649 Vermeij, G. J. 1975. Evolution and distribution of left-handed and planispiral coiling in snails.

650 Nature 254:419-420.
651 Whitlock, M. C. 2003. Fixation probability and time in subdivided populations. Genetics
652 164:767-779.
653
654
655

TABLES

Table 1. The diploid model without delayed inheritance ($h = 0$: a is a dominant allele, $h = 1$: A is a dominant allele)

Mating comb.	Mating prob.	AA	Aa	aa
AA × AA	x^2	1	0	0
AA × Aa	$2[1 - (1 - h)r]xy$	1/2	1/2	0
AA × aa	$2(1 - r)xz$	0	1	0
Aa × Aa	y^2	1/4	1/2	1/4
Aa × aa	$2(1 - hr)yz$	0	1/2	1/2
aa × aa	z^2	0	0	1

663 **FIGURE LEGENDS**

664 **Figure 1.** Chirality inheritance determined by maternal effects of dominant dextral (D) and
665 recessive sinistral (s) alleles at a single nuclear locus (delayed inheritance). Black and gray
666 spirals indicate dextral and sinistral phenotypes, respectively. In the second generation,
667 individuals of the same genotype (Ds) develop into the opposite enantiomorph depending on
668 the maternal genotype (DD or ss). Note that snails are androgynous.

669

670 **Figure 2.** Representative example for the trajectory of the fixation process of a mutant allele
671 that starts as a single heterozygote (black line) in the diploid model without delayed
672 inheritance. *X*-axis: frequency of the resident allele homozygotes, aa (z). *Y*-axis: frequency of
673 the mutant allele homozygotes, AA (x). Note that $x + z \leq 1$ (dashed line). The initial condition
674 is at $(z, x) = (1 - 1/N, 0)$ (black point). The gray curve ($x = 1 + z - 2\sqrt{z}$) indicates HW
675 equilibrium. Parameter values are $N = 30$, $r = 0.1$, $s = 0.1$, and $h = 1$.

676

677 **Figure 3.** Deterministic invasion conditions for a mutant allele. Invasion is possible above
678 each line. *X*-axis: reproductive isolation parameter (r). *Y*-axis: viability selection coefficient
679 (s). Completely recessive and dominant mutant alleles ($h = 0$ and 1) require a large selection

680 coefficient for invasion, whereas partially dominant alleles (e.g., h = 0.5) require a smaller
681 selection coefficient. Note that the invasion condition of the completely recessive mutant
682 allele differs from the limit of $h \to 0$ (dotted line).
683
684 **Figure 4.** Allele frequency dynamics affected by positive frequency-dependent selection due
685 to reproductive isolation (indicated by white arrows). Here is no viability selection (s = 0).
686 X-axis: mutant allele frequency (p). Y-axis: scaled derivatives of the mutant allele ($\dot{p}/r$). A:
687 The haploid model (solid gray line, eq. 8). An unstable equilibrium at p = 1/2 (white point)
688 divides two basins of attraction. Stable equilibria are at p = 0 and 1 (black points). B: The
689 diploid models with the dominant mutant allele without delayed inheritance (dotted red line,
690 eq. 11 when h = 1) and with delayed inheritance (solid red line, eq. 14). An unstable
691 equilibrium is at $p = 1-1/\sqrt{2}$. C: The diploid models with the recessive mutant allele
692 without delayed inheritance (dotted blue line, eq. 11 when h = 0) and with delayed inheritance
693 (solid blue line, eq. 15). An unstable equilibrium is at $p = 1/\sqrt{2}$. D: Comparison of the
694 diploid models with the dominant (red) and recessive (blue) alleles. Intersection points are at
695 $p = 1/2-\sqrt{3}/6$ and $1/2+\sqrt{3}/6$ (gray lines).
696

Figure 5. Relative fixation probabilities of a single mutant with reproductive isolation to that of a neutral mutant. Here is no viability selection ($s = 0$). A-F: X-axis is reproductive isolation parameter (r). G-I: X-axis is four times the product of reproductive isolation parameter and effective population size ($4Nr$). Y-axis is the product of fixation probability and effective population size ($N\rho$ in the haploid model and $2N\rho$ in the diploid models). A-C: $N = 3$ (first-step analyses and Monte Carlo simulations), D-F: $N = 10$ (Monte Carlo simulations), G-I: $N \to \infty$ (diffusion approximation) and $N = 1000$ (Monte Carlo simulations). A, D, G: Solid gray lines: the haploid model. B, C, E, F, H, I: Blue lines: the recessive mutant allele, red lines: the dominant mutant allele, green lines: the partial dominance model with two phenotypes ($h = 0.5$), solid lines: with delayed inheritance, dotted lines: without delayed inheritance. Points represent the results of Monte Carlo simulations. The solid gray line in Fig. 5G and the dotted green line in Fig. 5H are identical. The dotted blue and red lines (the diploid model without delayed inheritance) are overlapping in Fig. 5H. The solid blue and red lines (the diploid model with delayed inheritance) are overlapping in Fig. 5I.

Figure 6. The alleles with the highest fixation probabilities given certain strength of reproductive isolation and viability selection. Note that black lines do not represent invasion

714 conditions unlike Fig. 3. A: $N = 3$ (first-step analyses), B: $N = 10$ (Monte Carlo simulations),

715 C: $N \to \infty$ (diffusion approximation). A, B: X-axis is reproductive isolation parameter (r)

716 and Y-axis is viability selection coefficient (s). C: X-axis is four times the product of

717 reproductive isolation parameter and effective population size ($4Nr$) and Y-axis is four times

718 the product of viability selection coefficient and effective population size ($4Ns$). When $4Ns =$

719 0, both dominant and recessive mutant alleles with delayed inheritance have the same fixation

720 probability (dashed line). DI: delayed inheritance.

Online Supporting Information

Appendix S1: Invasion condition in the diploid model without delayed inheritance

We denote the frequencies of the genotypes, AA, Aa, and aa by x, y, and z (= 1 – x – y). The frequencies after mating are

$$\begin{aligned} T\mathcal{X} &= x^2 + \left[1-(1-h)r\right]xy + \frac{y^2}{4}, \\ T\mathcal{Y} &= \left[1-(1-h)r\right]xy + 2(1-r)xz + \frac{y^2}{2} + (1-hr)yz, \\ T\mathcal{Z} &= \frac{y^2}{4} + (1-hr)yz + z^2, \end{aligned} \tag{A1}$$

where $T = 1-2r\left[(1-h)xy + xz + hyz\right]$ is the sum of the frequencies of three genotypes after mating (see Table 1 for the derivation). The frequencies in the next generation after viability selection favoring a mutant phenotype is

$$\begin{aligned} x' &= \frac{(1+s)\mathcal{X}}{(1+s)\mathcal{X} + (1+hs)\mathcal{Y} + \mathcal{Z}}, \\ y' &= \frac{(1+hs)\mathcal{Y}}{(1+s)\mathcal{X} + (1+hs)\mathcal{Y} + \mathcal{Z}}, \\ z' &= \frac{\mathcal{Z}}{(1+s)\mathcal{X} + (1+hs)\mathcal{Y} + \mathcal{Z}}. \end{aligned} \tag{A2}$$

Here we assume that A is the mutant allele and a is the wild-type allele. When h = 1, the mutant allele is dominant; whereas, it is recessive when h = 0. We first consider the condition for the invasion of the completely or partially dominant mutant ($0 < h \le 1$). We then examine the invasibility condition for the completely recessive mutant ($h = 0$), in which we need to consult the center manifold theorem (Guckenheimer and Holmes 1983).

(i) Invasibility of the completely and partially dominant mutant ($0 < h \le 1$)

We linearize the dynamics (A2) for small x and y:

$$\begin{pmatrix} x' \\ y' \end{pmatrix} = \begin{pmatrix} 0 & 0 \\ 2(1-r)(1+hs) & (1+hs)(1-hr) \end{pmatrix} \begin{pmatrix} x \\ y \end{pmatrix} \tag{A3}$$

The largest eigenvalue of the linearized system is $(1+hs)(1-hr)$. Thus the mutant can invade if and only if $(1+hs)(1-hr) > 1$. This condition can be rewritten as $s > r/(1-hr)$.

(ii) Invasibility of the completely recessive mutant ($h = 0$)

If the mutant allele is completely recessive ($h=0$), the linearized system is also given by with $h=0$:

$$\begin{pmatrix} x' \\ y' \end{pmatrix} = A\begin{pmatrix} x \\ y \end{pmatrix} = \begin{pmatrix} 0 & 0 \\ 2(1-r) & 1 \end{pmatrix}\begin{pmatrix} x \\ y \end{pmatrix}. \tag{A4}$$

As the largest eigenvalue is 1, we need to have higher order terms of x and y to examine the local stability of $x=y=0$. The Taylor expansion of (A2) up to the quadratic terms of x and y yields

$$\begin{pmatrix} x' \\ y' \end{pmatrix} = \begin{pmatrix} 0 & 0 \\ 2(1-r) & 1 \end{pmatrix}\begin{pmatrix} x \\ y \end{pmatrix} + \begin{pmatrix} f(x,y) \\ g(x,y) \end{pmatrix}, \tag{A5}$$

with

$$\begin{aligned} f(x,y) &= (1+s)\left[x^2 + (1-r)xy + \frac{y^2}{4}\right], \\ g(x,y) &= -2(1-r)(1-2r)x^2 - (2-3r)xy - \frac{y^2}{2}. \end{aligned} \tag{A6}$$

The linear part of (A5) can be diagonalized by the transformation

$$\begin{pmatrix} x \\ y \end{pmatrix} = P\begin{pmatrix} u \\ v \end{pmatrix}, \text{ with } P = \begin{pmatrix} 0 & -\dfrac{1}{2(1-r)} \\ 1 & 1 \end{pmatrix}, \tag{A7}$$

where the column vectors of P are the eigenvectors corresponding to the eigenvalues 1 and 0 of matrix A. This yields

$$\begin{aligned} \begin{pmatrix} u' \\ v' \end{pmatrix} &= \begin{pmatrix} 1 & 0 \\ 0 & 0 \end{pmatrix}\begin{pmatrix} u \\ v \end{pmatrix} + P^{-1}\begin{pmatrix} f(x,y) \\ g(x,y) \end{pmatrix} \\ &\equiv \begin{pmatrix} 1 & 0 \\ 0 & 0 \end{pmatrix}\begin{pmatrix} u \\ v \end{pmatrix} + \begin{pmatrix} F(u,v) \\ G(u,v) \end{pmatrix}, \end{aligned} \tag{A8}$$

with

$$\begin{aligned} F(u,v) &= -\frac{1}{2}(r-s+rs)u^2 - \frac{r}{2(1-r)}uv + \frac{(2-r)r(1+s)}{2(1-r)}v^2, \\ G(u,v) &= -\frac{1}{2}(1-r)(1+s)u^2 - \frac{(2-r)r(1+s)}{2(1-r)}v^2. \end{aligned} \tag{A9}$$

Define the center manifold $W^c = \{(u,v) \mid v = k(u), k'(0) = k''(0) = 0\}$ on which the trajectory

near $u=v=0$ stays throughout the process. The simplest form would be $k(u)=au^2$. In order that the point (u',v') is also on the center manifold, we should have $v'=k(u')$. Substituting $u'=u+F(u,k(u))$ and $v'=G(u,k(u))$ into this yields

$$G(u,au^2)-a\left[u+F(u,au^2)\right]^2=0. \quad \text{(A10)}$$

Equating the coefficient of the leading term to zero, a is determined as

$$a=-\frac{1}{2}(1-r)(1+s). \quad \text{(A11)}$$

The slow dynamic of u restricted on the center manifold is then

$$u'=u+F(u,k(u))=u-\frac{1}{2}(r-s+rs)u^2, \quad \text{(A12)}$$

and hence u converges to zero if $r-s+rs>0$, or the mutant can invade if $r-s+rs<0$ (or $(1-r)(1+s)>1$). This invasibility condition for the completely recessive mutant is equivalent to that for the completely dominant mutant, but, interestingly, differs from the condition $s>r$ in the limit of $h\to 0$ for the invasibility condition of the partially dominant mutant.

Appendix S2: Invasion condition in the diploid model with delayed inheritance

In the presence of delayed inheritance, a phenotype of an individual is determined by a maternal genotype. We therefore need to keep track the frequencies of 2×3 combination of phenotype $\times$ genotype to describe the genetic dynamics. Here we denote the two alleles as A (dominant allele) and a (recessive allele). An individual has either phenotype A or a (right-handed or left-handed, depending on which is dominant) that is determined by the genotype of its mother. We denote for example an individual with the genotype AA and the phenotype A by AA_A.

As we assume that A is a dominant allele and a is a recessive allele in the diploid model with delayed inheritance, the genotype-phenotype combination AA_a will never be produced (indeed, for an individual to have phenotype a, its mother should be homozygote of the recessive allele, aa). We denote the frequencies of AA_A, Aa_A, Aa_a, aa_A, and aa_a as x_A, y_A, y_a, z_A, and z_a. $x_a\equiv 0$ as noted above. The frequency of phenotype A is $x_A+y_A+z_A$ and that of phenotype a is y_a+z_a. Let p_i $(=x_i+y_i/2)$ be the frequency of allele A with phenotype i $(=$A or a), and q_i $(z_i+y_i/2)$ be the frequency of allele a with phenotype i $(=$A or a). The frequencies after mating are calculated from Table S1 as

$$
\begin{aligned}
T\tilde{x}_{\mathrm{A}} &= (p_{\mathrm{A}}+p_{\mathrm{a}})^2 - 2rp_{\mathrm{A}}p_{\mathrm{a}},\\
T\tilde{y}_{\mathrm{A}} &= (p_{\mathrm{A}}+p_{\mathrm{a}})(q_{\mathrm{A}}+q_{\mathrm{a}}) + (p_{\mathrm{A}}+p_{\mathrm{a}})\frac{y_{\mathrm{A}}+y_{\mathrm{a}}}{2} - r(p_{\mathrm{A}}q_{\mathrm{a}}+p_{\mathrm{a}}q_{\mathrm{A}}) - \frac{r}{2}(p_{\mathrm{a}}y_{\mathrm{A}}+p_{\mathrm{A}}y_{\mathrm{a}}),\\
T\tilde{y}_{\mathrm{a}} &= (p_{\mathrm{A}}+p_{\mathrm{a}})(z_{\mathrm{A}}+z_{\mathrm{a}}) - r(p_{\mathrm{a}}z_{\mathrm{A}}+p_{\mathrm{A}}z_{\mathrm{a}}),\\
T\tilde{z}_{\mathrm{A}} &= (q_{\mathrm{A}}+q_{\mathrm{a}})\frac{y_{\mathrm{A}}+y_{\mathrm{a}}}{2} - \frac{r}{2}(q_{\mathrm{a}}y_{\mathrm{A}}+q_{\mathrm{A}}y_{\mathrm{a}}),\\
T\tilde{z}_{\mathrm{a}} &= (q_{\mathrm{A}}+q_{\mathrm{a}})(z_{\mathrm{A}}+z_{\mathrm{a}}) - r(q_{\mathrm{a}}z_{\mathrm{A}}+q_{\mathrm{A}}z_{\mathrm{a}}),
\end{aligned}
\qquad \text{(B1)}
$$

where $T = 1-2r(x_{\mathrm{A}}+y_{\mathrm{A}}+z_{\mathrm{A}})(y_{\mathrm{a}}+z_{\mathrm{a}})$. When there is no reproductive isolation (r = 0) or viability selection (s = 0), the ratio of two phenotypes for the heterozygous genotype, $\mathrm{Aa_A}$: $\mathrm{Aa_a}$, is (1 + p) : (1 – p) and that for the homozygous genotype, $\mathrm{aa_A}$: $\mathrm{aa_a}$, is p : (1 – p) under delayed inheritance assuming the HW equilibrium.

(i) Invasibility of a dominant mutant

The frequencies in the next generation are then given by those after the viability selection favoring a dominant handedness mutant (A) with the selection coefficient s:

$$
x'_{\mathrm{A}} = \frac{(1+s)\tilde{x}_{\mathrm{A}}}{W},\ y'_{\mathrm{A}} = \frac{(1+s)\tilde{y}_{\mathrm{A}}}{W},\ y'_{\mathrm{a}} = \frac{\tilde{y}_{\mathrm{a}}}{W},\ z'_{\mathrm{A}} = \frac{(1+s)\tilde{z}_{\mathrm{A}}}{W},\ z'_{\mathrm{a}} = \frac{\tilde{z}_{\mathrm{a}}}{W},
\qquad \text{(B1)}
$$

where $W = 1+s(\tilde{x}_{\mathrm{A}}+\tilde{y}_{\mathrm{A}}+\tilde{z}_{\mathrm{A}})$ is the mean fitness of the population.

We now examine the invasibility of the dominant allele A in the resident population consisting only of the recessive allele a (i.e., $z_{\mathrm{a}} = 1$ and $x_{\mathrm{A}} = y_{\mathrm{A}} = y_{\mathrm{a}} = z_{\mathrm{A}} = 0$). The system **Error! Reference source not found.**-(B1) is linearized with respect to z_{A}, y_{A}, y_{a}, and x_{A} as

$$
\begin{pmatrix} z'_{\mathrm{A}} \\ y'_{\mathrm{a}} \\ y'_{\mathrm{A}} \\ x'_{\mathrm{A}} \end{pmatrix} = \begin{pmatrix} 0 & (1+s)/2 & (1-r)(1+s)/2 & 0 \\ 0 & 1/2 & (1-r)/2 & 1-r \\ 0 & (1+s)/2 & (1-r)(1+s)/2 & (1-r)(1+s) \\ 0 & 0 & 0 & 0 \end{pmatrix} \begin{pmatrix} z_{\mathrm{A}} \\ y_{\mathrm{a}} \\ y_{\mathrm{A}} \\ x_{\mathrm{A}} \end{pmatrix},
\qquad \text{(B2)}
$$

where z_{a} is eliminated by using $z_{\mathrm{a}} = 1-x_{\mathrm{A}}-y_{\mathrm{A}}-y_{\mathrm{a}}-z_{\mathrm{A}}$. The Jacobian matrix in the right hand side of (B2) has three zero eigenvalues and a non-trivial eigenvalue,

$$
\lambda = \frac{1}{2}(2+s-r-rs).
\qquad \text{(B3)}
$$

The population allows the invasion of the dominant mutant if $\lambda > 1$, which gives exactly the same condition $(1-r)(1+s) > 1$ as that for the invasibility of dominant mutant if there was no delayed inheritance. Though the condition for the invasibility is the same, the value (B3)

itself is smaller than the dominant eigenvalue, $\lambda' = (1-r)(1+s)$, when there was no delayed inheritance, which corresponds to the fact that the delayed inheritance makes the invasion of a handedness mutant easier in a finite population.

(ii) Invasibility of a recessive mutant

Let us now consider the invasibility of a recessive handedness mutant that enjoys an ecological advantage in viability with the selection coefficient s. The frequencies after reproduction are given by **Error! Reference source not found.**, and the frequencies in the next generation are

$$x'_{\mathrm{A}} = \frac{\tilde{x}_{\mathrm{A}}}{W}, y'_{\mathrm{A}} = \frac{\tilde{y}_{\mathrm{A}}}{W}, y'_{\mathrm{a}} = \frac{(1+s)\tilde{y}_{\mathrm{a}}}{W}, z'_{\mathrm{A}} = \frac{\tilde{z}_{\mathrm{A}}}{W}, z'_{\mathrm{a}} = \frac{(1+s)\tilde{z}_{\mathrm{a}}}{W}, \tag{B4}$$

where $W = 1 + s(\tilde{y}_{\mathrm{a}} + \tilde{z}_{\mathrm{a}})$ is the mean fitness. As before $\tilde{x}_{\mathrm{a}} = 0$. The resident population consists only of dominant allele A (i.e., $x_{\mathrm{A}} = 1$ and $y_{\mathrm{A}} = y_{\mathrm{a}} = z_{\mathrm{A}} = z_{\mathrm{a}} = 0$). The system **Error! Reference source not found.**, (B4) is linearized with respect to z_{a}, z_{A}, y_{a}, and y_{A} as

$$\begin{aligned}
\begin{pmatrix} z'_{\mathrm{a}} \\ z'_{\mathrm{A}} \\ y'_{\mathrm{a}} \\ y'_{\mathrm{A}} \end{pmatrix} &= A \begin{pmatrix} z_{\mathrm{a}} \\ z_{\mathrm{A}} \\ y_{\mathrm{a}} \\ y_{\mathrm{A}} \end{pmatrix} + \begin{pmatrix} f_1(z_{\mathrm{a}}, z_{\mathrm{A}}, y_{\mathrm{a}}, y_{\mathrm{A}}) \\ f_2(z_{\mathrm{a}}, z_{\mathrm{A}}, y_{\mathrm{a}}, y_{\mathrm{A}}) \\ f_3(z_{\mathrm{a}}, z_{\mathrm{A}}, y_{\mathrm{a}}, y_{\mathrm{A}}) \\ f_4(z_{\mathrm{a}}, z_{\mathrm{A}}, y_{\mathrm{a}}, y_{\mathrm{A}}) \end{pmatrix} \\
&= \begin{pmatrix} 0 & 0 & 0 & 0 \\ 0 & 0 & 0 & 0 \\ (1-r)(1+s) & 1+s & 0 & 0 \\ 1-r & 1 & 1-r & 1 \end{pmatrix} \begin{pmatrix} z_{\mathrm{a}} \\ z_{\mathrm{A}} \\ y_{\mathrm{a}} \\ y_{\mathrm{A}} \end{pmatrix} + \begin{pmatrix} f_1(z_{\mathrm{a}}, z_{\mathrm{A}}, y_{\mathrm{a}}, y_{\mathrm{A}}) \\ f_2(z_{\mathrm{a}}, z_{\mathrm{A}}, y_{\mathrm{a}}, y_{\mathrm{A}}) \\ f_3(z_{\mathrm{a}}, z_{\mathrm{A}}, y_{\mathrm{a}}, y_{\mathrm{A}}) \\ f_4(z_{\mathrm{a}}, z_{\mathrm{A}}, y_{\mathrm{a}}, y_{\mathrm{A}}) \end{pmatrix},
\end{aligned} \tag{B5}$$

where f_i's are quadratic or higher order terms of z_{a}, z_{A}, y_{a}, and y_{A}. The matrix A has eigenvalues $\lambda = 1$ and $\lambda = 0$ (with multiplicity 3). Because the dominant eigenvalue is 1, we need to construct a center manifold to examine the local stability of the equilibrium $(z_{\mathrm{a}}, z_{\mathrm{A}}, y_{\mathrm{a}}, y_{\mathrm{A}})^T = (0,0,0,0)^T$, where superscript T denotes the vector transform.

The eigenvector corresponding to the eigenvalue 1 is found, by solving $(A - 1I)\mathbf{b} = \mathbf{0}$, to be $\mathbf{b}_1 = (1,0,0,0)^T$, where I is a 4×4 identity matrix. There are two eigenvectors satisfying $(A - 0I)\mathbf{b} = A\mathbf{b} = \mathbf{0}$ corresponding to the eigenvalue 0:

115 $$\mathbf{b}_2 = \begin{pmatrix} 1 \\ -(1-r) \\ 0 \\ 0 \end{pmatrix}, \text{ and } \mathbf{b}_3 = \begin{pmatrix} 0 \\ 0 \\ 1 \\ -(1-r) \end{pmatrix}. \quad \text{(B6)}$$

116 We now find a nonzero vector $\mathbf{b}_4$ that, together with $\mathbf{b}_2$ and $\mathbf{b}_3$, spans the 3-dimensional
117 generalized eigenspace corresponding to the eigenvalue 0. Such vector $\mathbf{b}_4$ must satisfy
118 $(A-0I)^2\mathbf{b}_4 = A^2\mathbf{b}_4 = \mathbf{0}$ and be linearly independent of $\mathbf{b}_2$ or $\mathbf{b}_3$, which is obtained as

119 $$\mathbf{b}_4 = \begin{pmatrix} 1 \\ 0 \\ 0 \\ -(1-r)(2+s-r-rs) \end{pmatrix}. \quad \text{(B7)}$$

120 Now we define the transformation matrix P whose columns consist of $\mathbf{b}_1$, $\mathbf{b}_2$, $\mathbf{b}_3$, and
121 $\mathbf{b}_4$:

122 $$P = \begin{pmatrix} 0 & 1 & 0 & 1 \\ 0 & -(1-r) & 0 & 0 \\ 0 & 0 & 1 & 0 \\ 1 & 0 & -(1-r) & -(1-r)(2+s-r-rs) \end{pmatrix}. \quad \text{(B8)}$$

123 We then transform the variables as

124 $$\begin{pmatrix} z_{\mathrm{a}} \\ z_{\mathrm{A}} \\ y_{\mathrm{a}} \\ y_{\mathrm{A}} \end{pmatrix} = P \begin{pmatrix} u_1 \\ u_2 \\ u_3 \\ u_4 \end{pmatrix}. \quad \text{(B9)}$$

125 The dynamics for the transformed variables become

$$
\begin{aligned}
\begin{pmatrix} u_1' \\ u_2' \\ u_3' \\ u_4' \end{pmatrix} &= P^{-1}AP\begin{pmatrix} u_1 \\ u_2 \\ u_3 \\ u_4 \end{pmatrix} + P^{-1}\begin{pmatrix} f_1 \\ f_2 \\ f_3 \\ f_4 \end{pmatrix} \\
&= \begin{pmatrix} 1 & 0 & 0 & 0 \\ 0 & 0 & 0 & 0 \\ 0 & 0 & 0 & (1-r)(1+s) \\ 0 & 0 & 0 & 0 \end{pmatrix}\begin{pmatrix} u_1 \\ u_2 \\ u_3 \\ u_4 \end{pmatrix} + \begin{pmatrix} F_1(u_1,u_2,u_3,u_4) \\ F_2(u_1,u_2,u_3,u_4) \\ F_3(u_1,u_2,u_3,u_4) \\ F_4(u_1,u_2,u_3,u_4) \end{pmatrix}.
\end{aligned} \tag{B10}
$$

Here, $F_i(u_1,u_2,u_3,u_4)$ is the ith row of $P^{-1}\mathbf{f}(\mathbf{x}) = P^{-1}\mathbf{f}(P\mathbf{u})$ where $\mathbf{f} = (f_1, f_2, f_3, f_4)^T$, $\mathbf{x} = (z_a, z_A, y_a, y_A)^T$, and $\mathbf{u} = (u_1,u_2,u_3,u_4)^T$. We now define the center manifold

$$
W^c = \left\{(u_1,u_2,u_3,u_4) \,|\, u_2 = f(u_1), u_3 = g(u_1), u_4 = h(u_1)\right\}, \tag{B11}
$$

where f, g, and h are functions with the following properties: $f(0) = g(0) = h(0) = 0$ and $f'(0) = g'(0) = h'(0) = 0$. The simplest forms for such functions are $f(u) = au^2$, $g(u) = bu^2$, and $h(u) = cu^2$ where a, b, and c are constants. Substituting these into (B10), and requiring that the variables u_2', u_3', and u_4' in the next generation must lie on the center manifold ($u_2' = f(u_1')$, $u_3' = g(u_1')$, and $u_4' = h(u_1')$), we now have

$$
\begin{aligned}
u_1' &= u_1 + F_1(u_1, au_1^2, bu_1^2, cu_1^2), \\
a\left[u_1 + F_1(u_1, au_1^2, bu_1^2, cu_1^2)\right]^2 &= F_2(u_1, au_1^2, bu_1^2, cu_1^2), \\
b\left[u_1 + F_1(u_1, au_1^2, bu_1^2, cu_1^2)\right]^2 &= (1-r)(1+s)cu_1^2 + F_3(u_1, au_1^2, bu_1^2, cu_1^2), \\
c\left[u_1 + F_1(u_1, au_1^2, bu_1^2, cu_1^2)\right]^2 &= F_4(u_1, au_1^2, bu_1^2, cu_1^2).
\end{aligned} \tag{B12}
$$

The coefficients a, b, and c are determined from the leading order terms of the second to the forth equations of (B12) as

$$
a = -\frac{1}{4(1-r)}, \quad b = \frac{1+s}{4}, \quad c = \frac{1}{4(1-r)}. \tag{B13}
$$

Substituting this into the first equation of (B12), we have a slow dynamics on the center manifold:

$$u_1' = u_1 + \frac{1}{4}(s - r - rs)u_1^2 + O\left(u_1^3\right). \tag{B14}$$

Thus, u_1 converges to zero if and only if $s(1-r) - r < 0$ or $s < r/(1-r)$. Conversely, the recessive mutant can invade the population if $s > r/(1-r)$. This condition is the same as the condition $(2 + s - r - rs)/2 > 1$ or $(1-r)(1+s) > 1$ for the invasibility of the dominant mutant.

The center manifold $u_2 = -u_1^2/\left[4(1-r)\right]$, $u_3 = (1+s)u_1^2/4$, and $u_4 = u_1^2/\left[4(1-r)\right]$ in the original coordinate is defined in a parametric form with a parameter $\xi = u_1$ as

$$\begin{aligned} z_a &= O\left(\xi^3\right), \\ z_A &= \frac{1}{4}\xi^2 + O\left(\xi^3\right), \\ y_a &= \frac{1+s}{4}\xi^2 + O\left(\xi^3\right), \\ y_A &= \xi - \frac{3 + 2s - 2r - 2rs}{4}\xi^2 + O\left(\xi^3\right). \end{aligned} \tag{B15}$$

Appendix S3: Diffusion approximation analysis of the diploid model without delayed inheritance

We here derive the approximate one-dimensional diffusion process describing the allele frequency dynamics in a finite population of effective population size *N* without delayed inheritance. The discrete-generation genotype dynamics in infinite population are derived as (A1)-(A2) of Appendix S1. As is usual in diffusion approximation, we take the limit of weak fecundity and viability selections, $r \to 0$, $s \to 0$, and large population $N \to \infty$ with the products *Nr* and *Ns* being kept finite.

Assuming that both *s* and *r* are of the order of ε, a small positive constant, we expand the dynamics (A1)-(A2) in Taylor series with respect to ε. The leading order dynamics for the zygote frequencies *x*, *y*, and *z* of genotypes AA, Aa, and aa are then

$$\begin{aligned} x' &= p^2 + O(\varepsilon), \\ y' &= 2pq + O(\varepsilon), \\ z' &= q^2 + O(\varepsilon), \end{aligned} \tag{C1}$$

where $p = x + y/2$ and $q = z + y/2$ respectively is the frequency of allele A and a. Thus, in the leading order, genotype frequencies are in the Hardy-Weinberg equilibrium. From this it

also follows that the allele frequencies do not change with time, $p' = p$ and $q' = q$, up to the leading order.

Now we derive the slow allele frequency dynamics as the first order expansion of the equations (A1) and (A2). The change in the allele frequency p of the mutant allele A is then

$$\Delta p = p(1-p)\left\{r\left[p(2p^2-1)-h(6p^2-6p+1)\right]+s\left[p+h(1-2p)\right]\right\}+O(\varepsilon^2). \quad \text{(C2)}$$

Note that s in (C2) is the selection coefficient favoring the phenotype A. From (C2) we have the frequency dynamics:

$$\dot{p} = p(1-p)\left\{r\left[p(2p^2-1)-h(6p^2-6p+1)\right]+s\left[p+h(1-2p)\right]\right\}. \quad \text{(C3)}$$

The dynamics has two stable equilibria at p = 0 and p = 1, and an internal unstable equilibrium when $r > s$.

With random genetic drift, the diffusion process for the change in the allele frequency is characterized by infinitesimal mean and variance of the frequency change:

$$M(p) = E\left[\Delta p \middle| p\right] = p(1-p)\left\{r\left[p(2p^2-1)-h(6p^2-6p+1)\right]+s\left[p+h(1-2p)\right]\right\},$$
$$V(p) = E\left[(\Delta p)^2 \middle| p\right] = \frac{p(1-p)}{2N}. \quad \text{(C4)}$$

The fixation probability of the allele A with the initial frequency p then satisfies the backward equation (12) with the boundary condition $u(0) = 0$ and $u(1) = 1$. This yields equation (13). The fixation probability of a single mutant $\rho = u(1/2N)$ is then

$$\rho = \frac{1/(2N)}{\int_0^1 \exp\left\{4Nry(1-y)\left[\frac{y}{2}(1+y)-h(2y-1)\right]-4Nsy\left[\frac{y}{2}+h(1-y)\right]\right\}dy}, \quad \text{(C5)}$$

The relative fixation rate of a single mutant relative to that of a neutral mutant is given by $\phi = 2N\rho$:

$$\phi = \frac{1}{\int_0^1 \exp\left\{Ry(1-y)\left[\frac{y}{2}(1+y)-h(2y-1)\right]-Sy\left[\frac{y}{2}+h(1-y)\right]\right\}dy}, \quad \text{(C6)}$$

where $R = 4Nr$ and $S = 4Ns$. Here we consider three cases: (i) h = 0 (the recessive mutant), (ii) h = 1 (the dominant mutant), (iii) h = 0.5 (the partially dominant mutant).

(i) *h* = 0 (the recessive mutant)

After factorization, the deterministic dynamics is

$$\dot{p} = p^2(1-p)\left[r(2p^2-1)+s\right], \tag{C7}$$

when $h = 0$. This can be written as

$$\dot{p} = 2rp^2(1-p)\left(p-\sqrt{\frac{r-s}{2r}}\right)\left(p+\sqrt{\frac{r-s}{2r}}\right),$$

when $r > 0$ and $r > s$. Thus the dynamics has an internal unstable equilibrium at $p_c = \sqrt{(r-s)/2r}$ when $r > s$. When $s = 0$, therefore, the dynamics has two stable equilibria at $p = 0$ and $p = 1$, and an internal unstable equilibrium at $p_c = 1/\sqrt{2}$ (the dotted blue line in Fig. 3).

The relative fixation rate is

$$\phi_0 = \frac{1}{\int_0^1 \exp\left\{\frac{y^2}{2}\left[R(1-y^2)-S\right]\right\}dy}. \tag{C8}$$

When $s = 0$, for the relative fixation rate, $\phi_0 = 1/\int_0^1 \exp\left[\frac{Ry^2}{2}(1-y^2)\right]dy$, we can show the following properties. Firstly, at the limit of $R \to 0$ the fixation probability is equal to that of a neutral allele:

$$\phi_0\big|_{R=0} = 1. \tag{C9}$$

Secondly we see that $1/\phi_0$ is convex with respect to R because

$$\frac{\partial^2}{\partial R^2}\left(\frac{1}{\phi_0}\right) = \frac{1}{4}\int_0^1 \left(y^2-y^4\right)^2 \exp\left[\frac{R}{2}\left(y^2-y^4\right)\right]dy > 0. \tag{C10}$$

Thirdly we see that the sign of the initial slope of $1/\phi_0$ from

$$\left.\frac{\partial}{\partial R}\left(\frac{1}{\phi_0}\right)\right|_{R=0} = \frac{1}{15}. \tag{C11}$$

Because the right-hand side of equation (C11) is positive, ϕ_0 is smaller than 1 for any $R > 0$. The fixation probability of a dominant mutant allele is always smaller than that, $1/(2N)$, of a neutral allele (i.e. the native recessive allele is the finite population size ESS, ESS_N, in the sense of Nowak et al. (2004)). In addition, this value is smaller than the haploid model (1/12), implying that the reduction rate of fixation probability is more moderate in the diploid model.

(ii) *h* = 1 (the dominant mutant)

The frequency dynamics of dominant mutant is obtained from equation (C3):

$$\dot{p} = p(1-p)^2\left[-r\left(2p^2-4p+1\right)+s\right]. \qquad \text{(C12)}$$

This can be written as

$$\dot{p} = 2rp(1-p)^2\left[p-\left(1-\sqrt{\frac{r+s}{2r}}\right)\right]\left[\left(1+\sqrt{\frac{r+s}{2r}}\right)-p\right].$$

If $r > s$, this has an internal unstable equilibrium at $p_c = 1-\sqrt{(r+s)/2r}$. When $s = 0$, the dynamics has an internal unstable equilibrium at $p_c = 1-1/\sqrt{2}$ (the dotted red line in Fig. 3).

Therefore the relative fixation rate of a recessive mutant to that of a neutral allele $\phi_1 = 2N\rho_1$ then satisfies

$$\phi_1 = \frac{1}{\int_0^1 \exp\left\{-\left(2-y\right)\left[R(1-y)^2-S\right]\right\}dy}. \qquad \text{(C13)}$$

If $s = 0$, we can show that the function $(1/\phi_1)$ is convex with respect to R, $\phi_1\big|_{R=0} = 1$, and $\left(\partial(1/\phi_1)/\partial R\right)\big|_{R=0} = 1/15$. Actually, ϕ_1 and ϕ_0 are equivalent ($\phi_0 = \phi_1$) when $s = 0$, though it is different when $s > 0$. This is obvious from equations (C8) and (C13); if we represent the frequency of the recessive allele as p and that of the dominant allele as q, then

$$\begin{aligned} p^2\left(1-p^2\right) &= (1-q)^2\left[1-(1-q)^2\right] \\ &= q(2-q)(1-q)^2. \end{aligned} \qquad \text{(C14)}$$

(iii) *h* = 0.5 (the partially dominant mutant)

The frequency dynamics of mutant with partial dominance is obtained from equation (C3):

$$\dot{p} = \frac{1}{2}p(1-p)\left[r\left(2p-1\right)\left(2p^2-2p+1\right)+s\right]. \qquad \text{(C15)}$$

This has an internal unstable equilibrium at

$$p_c = \frac{1}{2}+\frac{1}{2}\left(\sqrt{\frac{1}{27}+\left(\frac{s}{r}\right)^2}-\frac{s}{r}\right)^{\frac{1}{3}}-\frac{1}{6}\left(\sqrt{\frac{1}{27}+\left(\frac{s}{r}\right)^2}-\frac{s}{r}\right)^{-\frac{1}{3}},$$

when $r > s$. Equation (C15) has an internal unstable equilibrium at $p_c = 1/2$ when $s = 0$ (the dotted lime-green line in Fig. S1). The relative fixation rate is

$$\phi_2 = \frac{1}{\int_0^1 \exp\left\{-\left[R(1-2y+2y^2-y^3)-S\right]\right\}dy}. \qquad \text{(C16)}$$

If $s = 0$, we can show that the function $(1/\phi_2)$ is convex with respect to R, $\phi_2\big|_{R=0} = 1$, and $\left(\partial(1/\phi_2)/\partial R\right)\big|_{R=0} = 1/15$.

These analytical expressions for the relative fixation rates ϕ_0, ϕ_1 and ϕ_2 obtained from one-dimensional diffusion approximation showed good agreements with the simulation results when N = 1,000 (Fig. 4H). When s = 0, we found that ϕ_0 and ϕ_1 are equivalent as shown in equation (C14) (Fig. 4H) and that ϕ_2 is higher than ϕ_0 and ϕ_1 when R is not small, implying that partial dominance can promote fixation of the mutant allele in the diploid model with three phenotypes (Figs. 4H, S2C).

Appendix S4: Diffusion approximation analysis of the diploid model with delayed inheritance

We here derive the approximate one-dimensional diffusion process describing the allele frequency dynamics of snail handedness alleles in a finite population of effective population size N with delayed inheritance. The discrete-generation genotype-phenotype dynamics in infinite population are derived as (B1) and (B2) or (B1) and (B5) of Appendix S2. As is usual in diffusion approximation, we take the limit of weak fecundity and viability selections, $r \to 0$, $s \to 0$, and large population $N \to \infty$ with the products Nr and Ns being kept finite.

Assuming that both s and r are of the order of ε, a small positive constant, we expand the dynamics (B1) and (B2)/(B5) in Taylor series with respect to ε. The leading order dynamics for the zygote frequencies $x = x_A + x_a$, $y = y_A + y_a$, $z = z_A + z_a$ of genotypes AA, Aa, and aa are then

$$\begin{aligned} x' &= p^2 + O(\varepsilon), \\ y' &= 2pq + O(\varepsilon), \\ z' &= q^2 + O(\varepsilon), \end{aligned} \qquad \text{(D1)}$$

where $p = x + y/2$ and $q = z + y/2$ respectively is the frequency of allele A and a. Thus, in the leading order, genotype frequencies are in the Hardy-Weinberg equilibrium. From this it

also follows that the allele frequencies do not change with time, $p' = p$ and $q' = q$, up to the leading order. The frequencies of phenotype-genotype combinations are thus kept constant for a given allele frequency p (or q) up to the leading order:

$$\begin{aligned} x_{\mathrm{A}} &= p^2 + O(\varepsilon), \\ x_{\mathrm{a}} &= 0, \\ y_{\mathrm{A}} &= pq(1+p) + O(\varepsilon), \\ y_{\mathrm{a}} &= pq^2 + O(\varepsilon), \\ z_{\mathrm{A}} &= pq^2 + O(\varepsilon), \\ z_{\mathrm{a}} &= q^3 + O(\varepsilon). \end{aligned} \tag{D2}$$

Now we derive the slow allele frequency dynamics as the first order expansion of the equations (B1) and (B2)/(B5). The change in the allele frequency p of the dominant allele A is then

$$\Delta p = \frac{1}{2} p(1-p)^2 \left[-r(2p^2 - 4p + 1) - s \right] + O(\varepsilon^2). \tag{D3}$$

For the frequency q of the recessive allele, we have

$$\Delta q = \frac{1}{2} q^2 (1-q) \left[r(2q^2 - 1) + s \right] + O(\varepsilon^2). \tag{D4}$$

Note that s in (D3) and (D4) is the selection coefficient favoring phenotype a. If phenotype A is selected for, the sign must be changed before s in the right hand side of (D3) and (D4).

(i) The dominant mutant alleles

If the dominant mutant is selected for in the viability selection, we change the sign before s in the right hand side of (D3) to have the deterministic dynamics,

$$\dot{p} = \frac{1}{2} p(1-p)^2 \left[-r(2p^2 - 4p + 1) + s \right]. \tag{D5}$$

This rate of change in the allele frequency of dominant allele is exactly a half of that for the diploid model without delayed inheritance with $h = 1$ (eq. C12). In other words, the delayed inheritance does not change allele frequency dynamics at all except for its halved rate. Therefore, the position of internal unstable equilibrium, $p_c = 1 - 1/\sqrt{2}$, is the same as in the model without delayed inheritance (the solid red line in Fig. 3).

The relative fixation rate of a dominant mutant to that of a neutral allele $\phi_{\mathrm{A}} = 2N\rho_{\mathrm{A}}$ then satisfies

$$\phi_{\mathrm{A}} = \frac{1}{\int_0^1 \exp\left\{\frac{y}{4}(2-y)\left[R(1-y)^2 - S\right]\right\} dy}. \qquad \text{(D6)}$$

(ii) The recessive mutant allele

If the recessive allele is selected for in the viability selection, we have from (D4) the deterministic dynamics,

$$\dot{q} = \frac{1}{2}q^2(1-q)\left[r(2q^2-1)+s\right]. \qquad \text{(D7)}$$

Again, the right hand side is exactly a half of that for the diploid model without delayed inheritance with $h = 0$ (eq. C7). Thus, two stable equilibria at $q = 0$ and $q = 1$, and an internal unstable equilibrium at $q_c = 1/\sqrt{2}$ are exactly the same as in the model without delayed inheritance (the solid blue line in Fig. 3). The relative fixation rate of a recessive mutant to that of a neutral allele $\phi_{\mathrm{a}} = 2N\rho_{\mathrm{a}}$ then satisfies

$$\phi_{\mathrm{a}} = \frac{1}{\int_0^1 \exp\left\{\frac{z^2}{4}\left[R(1-z^2)-S\right]\right\} dz}. \qquad \text{(D8)}$$

Note that ϕ_{A} and ϕ_{a} are equivalent when $s = 0$, which can be shown by changing the variables in the integral in (D8) from z to $y = 1 - z$. When $s = 0$, the initial slope of $1/\phi_{\mathrm{A}}$ and $1/\phi_{\mathrm{a}}$ is $\left(\partial(1/\phi_{\mathrm{A}})/\partial R\right)_{R=0} = 1/30$. This value is smaller than the haploid model (1/12) and the diploid model without delayed inheritance (1/15), implying that the reduction rate of fixation probability is more moderate in the diploid model with delayed inheritance.

The analytical formula for the relative fixation probabilities, (D6) and (D8), by one dimensional diffusion approximation showed good agreements with the Monte Carlo simulation results for the original 4 dimensional genotype-phenotype dynamics for sufficiently large N ($N = 1{,}000$, Fig. 4I).

Appendix S5: Exact fixation probabilities in the haploid model

We calculated exact fixation probabilities in the Markov process without any approximation by the first step analysis. Consider a finite population with N haploid individuals. Recursion equations of fixation probabilities can be written as

316 $$u(i) = \sum_{j=0}^{N} P_{i,j} u(j), \qquad \text{(E1)}$$

317 where $u(i)$ is the probability that a mutant allele starting with i individuals in the initial
318 population eventually goes to fixation, and $P_{i,j}$ is the transition probability that the number of
319 mutant allele change from i to j in one generation ($0 \le i, j \le N$). Note that u here is a function
320 of number of individuals, but u in Appendix S3 and S4 is a function of frequencies. With the
321 boundary conditions $u(0) = 0$ and $u(N) = 1$, the fixation probability can be obtained by solving
322 linear equations with $N - 1$ unknown variables. This can be written in a matrix form:

323 $$A\mathbf{u} = \mathbf{b}, \qquad \text{(E2)}$$

324 where

$$A = \begin{pmatrix} P_{1,1} - 1 & P_{1,2} & \mathsf{L} & P_{1,(N-1)} \\ P_{2,1} & P_{2,2} - 1 & \mathsf{L} & P_{2,(N-1)} \\ \mathsf{M} & \mathsf{M} & \mathsf{O} & \mathsf{M} \\ P_{(N-1),1} & P_{(N-1),2} & \mathsf{L} & P_{(N-1),(N-1)} - 1 \end{pmatrix},$$

325 $$\mathbf{u} = \begin{pmatrix} u(1) \\ u(2) \\ \mathsf{M} \\ u(N-1) \end{pmatrix},$$

$$\mathbf{b} = \begin{pmatrix} -P_{1,N} \\ -P_{2,N} \\ \mathsf{M} \\ -P_{(N-1),N} \end{pmatrix}.$$

326 The solution can be obtained by multiplying the inverse of matrix A in the both sides of
327 (E1): $\mathbf{u} = A^{-1}\mathbf{b}$. The transition probability $P_{i,j}$ is given by the binomial distribution when
328 there is no selection ($r = s = 0$):

329 $$P_{i,j} = \binom{N}{j} p^j (1-p)^{N-j}, \qquad \text{(E3)}$$

330 where $p = i/N$. When there is positive frequency-dependent selection due to reproductive
331 isolation ($r > 0$ and $s = 0$), the expected frequency in the next generation in equation (E3), p,
332 is replaced by equation (1):

333 $$P_{i,j} = \binom{N}{j} \left(\frac{p[1 - r(1-p)]}{1 - 2rp(1-p)} \right)^j \left(1 - \frac{p[1 - r(1-p)]}{1 - 2rp(1-p)} \right)^{N-j}. \qquad \text{(E4)}$$

When there is viability selection for the mutant ($r > 0$ and $s > 0$), equation (E3) is replaced by

$$P_{i,j} = \binom{N}{j} \left(\frac{(1+s)\tilde{p}}{1+s\tilde{p}} \right)^{j} \left(1 - \frac{(1+s)\tilde{p}}{1+s\tilde{p}} \right)^{N-j}, \qquad \text{(E5)}$$

where $\tilde{p}$ is from equation (1). The graphs of $u(1)$ are in good agreement with the simulation results when $N = 3$ (Fig. 4A).

One drawback of this method is that calculating the inverse matrix of the transition probability matrix, A, is time-consuming or almost impossible when N is large. In the diploid models, the dimension is two without delayed inheritance and four with delayed inheritance. Due to the 'curse of dimensionality,' therefore, calculation is especially difficult in the diploid models. For sufficiently small population size, however, this method is practical and gives accurate results for very small N when diffusion approximation fails.

Appendix S6: Exact fixation probabilities in the diploid model without delayed inheritance

Consider a finite population with diploid N individuals. The fixation probability can be calculated as

$$u(i,j) = \sum_{k=0}^{N} \sum_{l=0}^{N} P_{ij,kl} u(k,l), \qquad \text{(F1)}$$

where $u(i, j)$ is the fixation probability when there are i individuals of AA homozygote and j individuals of aa homozygote (we call this as state (i, j) hereafter) and $P_{ij,kl}$ is the transition probability from state (i, j) to state (k, l) in one generation ($0 \le i, j, k, l \le N$). Note that the number of heterozygous individuals Aa is $(N - i - j)$ or $(N - k - l)$. With the boundary conditions $u(0, N) = 0$ and $u(N, 0) = 1$ where the mutant allele is A and the wild-type allele is a, the fixation probability of a mutant allele, $u(0, N - 1)$, can be obtained by solving linear equations for $(N+1)(N+2)/2-2$ unknowns $u(i, j)$ for $i = 0,1,\cdots,N-1$, $j = 0,1,\cdots,N-1$, with $i + j \le N$. This can be rewritten in a matrix form $A\mathbf{u} = \mathbf{b}$:

$$\begin{pmatrix} P_{00,00}-1 & P_{00,01} & \cdots & P_{00,(N-1)1} \\ P_{01,00} & P_{01,01}-1 & \cdots & P_{01,(N-1)1} \\ \vdots & \vdots & \ddots & \vdots \\ P_{(N-1)1,00} & P_{(N-1)1,01} & \cdots & P_{(N-1)1,(N-1)1}-1 \end{pmatrix} \begin{pmatrix} u(0,0) \\ u(0,1) \\ \vdots \\ u(N-1,1) \end{pmatrix} = \begin{pmatrix} -P_{00,N0} \\ -P_{01,N0} \\ \vdots \\ -P_{(N-1)1,N0} \end{pmatrix}.$$

The solution is obtained by multiplying the inverse of matrix A in the both sides: $\mathbf{u} = A^{-1}\mathbf{b}$. The transition probability is given by the multinomial distribution,

$$P_{ij,kl} = \frac{N!}{k!(N-k-l)!l!}\left[\left(x+\frac{y}{2}\right)^2\right]^k\left[2\left(x+\frac{y}{2}\right)\left(\frac{y}{2}+z\right)\right]^{N-k-l}\left[\left(\frac{y}{2}+z\right)^2\right]^l, \quad \text{(F2)}$$

where $x = i/N$, $y = 1 - (i + j)/N$, and $z = j/N$. When there is positive frequency-dependent selection due to reproductive isolation or viability selection for the mutant in addition to reproductive isolation, the expected frequencies of genotypes in the next generation in equation (F2) is replaced by equation (A1) or (A2).

Appendix S7: Exact fixation probabilities in the diploid model with delayed inheritance

Consider a finite population with diploid N individuals. The fixation probability can be calculated as

$$u(a,b,c,d) = \sum_{i=0}^{N}\sum_{j=0}^{N}\sum_{k=0}^{N}\sum_{l=0}^{N} P_{abcd,ijkl}\,u(i,j,k,l), \quad \text{(G1)}$$

where $u(a, b, c, d)$ is the fixation probability when there are a individuals of AA_A, b individuals of Aa_A, c individuals of Aa_a, and d individuals of aa_A (we call this as state (a, b, c, d) hereafter) and $P_{abcd,ijkl}$ is the transition probability from state (a, b, c, d) to state (i, j, k, l) in one generation ($0 \le a, b, c, d, i, j, k, l \le N$). Note that the number of aa_a individuals is ($N - a - b - c - d$) or ($N - i - j - k - l$). The frequencies of AA_A, Aa_A, Aa_a, and aa_A are x_A (= a/N), y_A (= b/N), y_a (= c/N), z_A (= d/N). With the boundary conditions $u(0, 0, 0, 0) = u(0, 0, 0, 1) = \ldots = u(0, 0, 0, N) = 0$ and $u(N, 0, 0, 0) = 1$ where the dominant mutant allele is A and the recessive wild-type allele is a, the fixation probability of a mutant allele, $u(0, 0, 1, 0)$, can be obtained by solving linear equations for $u(i,j,k,l)$ with $i,j,k,l = 0,1,\cdots,N$ and $i+j+k+l \le N$. This can be rewritten in a matrix form $A\mathbf{u} = \mathbf{b}$:

$$\begin{pmatrix} P_{1000,1000}-1 & P_{1000,2000} & \cdots & P_{1000,00N0} \\ P_{2000,1000} & P_{2000,2000}-1 & \cdots & P_{2000,00N0} \\ \vdots & \vdots & \ddots & \vdots \\ P_{00N0,1000} & P_{00N0,2000} & \cdots & P_{00N0,00N0}-1 \end{pmatrix}\begin{pmatrix} u(1,0,0,0) \\ u(2,0,0,0) \\ \vdots \\ u(0,0,N,0) \end{pmatrix} = \begin{pmatrix} -P_{1000,N000} \\ -P_{2000,N000} \\ \vdots \\ -P_{00N0,N000} \end{pmatrix}.$$

The solution is obtained as: $\mathbf{u} = A^{-1}\mathbf{b}$. The transition probability is given by the multinomial distribution,

$$P_{abcd,ijkl} = \frac{N!}{i!j!k!l!(N-i-j-k-l)!}\bar{x}_A^i\bar{y}_A^j\bar{y}_a^k\bar{z}_A^l\left(1-\bar{x}_A-\bar{y}_A-\bar{y}_a-\bar{z}_A\right)^{N-i-j-k-l}, \quad \text{(G2)}$$

where

$$\overline{x}_{\mathrm{A}} = \left(\frac{a}{N} + \frac{b+c}{2N}\right)^2,$$
$$\overline{y}_{\mathrm{A}} = \left(\frac{a}{N} + \frac{b+c}{2N}\right)\left(1 - \frac{a}{N}\right),$$
$$\overline{y}_{\mathrm{a}} = \left(\frac{a}{N} + \frac{b+c}{2N}\right)\frac{d+e}{N},$$
$$\overline{z}_{\mathrm{A}} = \frac{b+c}{2N}\left(\frac{b+c}{2N} + \frac{d+e}{N}\right).$$

388

389 The expected frequencies in the next generation in equation (G2) are replaced by equations
390 (B1)-(B2) when there is positive frequency-dependent selection due to reproductive isolation
391 and viability selection for the mutant.

392 When the recessive mutant allele is a and the wild-type allele is A, we solved the
393 equation,

394
$$\begin{pmatrix} P_{1000,1000}-1 & P_{1000,2000} & \mathsf{L} & P_{1000,00N0} \\ P_{2000,1000} & P_{2000,2000}-1 & \mathsf{L} & P_{2000,00N0} \\ \mathsf{M} & \mathsf{M} & \mathsf{O} & \mathsf{M} \\ P_{00N0,1000} & P_{00N0,2000} & \mathsf{L} & P_{00N0,00N0}-1 \end{pmatrix}\begin{pmatrix} u(1,0,0,0) \\ u(2,0,0,0) \\ \mathsf{M} \\ u(0,0,N,0) \end{pmatrix} = \begin{pmatrix} -P_{1000,0000} \\ -P_{2000,0000} \\ \mathsf{M} \\ -P_{00N0,0000} \end{pmatrix},$$

395 to obtain the fixation probability of a single mutant, $u(N - 1, 1, 0, 0)$, with the boundary
396 conditions: $u(N, 0, 0, 0) = 0$ and $u(0, 0, 0, 0) = u(0, 0, 0, 1) = \ldots = u(0, 0, 0, N) = 1$. The
397 expected frequencies in the next generation in equation (G2) are replaced by equations (B1)
398 and (B5) when there is positive frequency-dependent selection due to reproductive isolation
399 and viability selection for the mutant.

400

401

402 **Appendix S8: The partial dominance model with two phenotypes**

403 Thus far we considered the model in which h is a parameter that determines the intermediate
404 phenotype of heterozygote (Appendix S1, S3). Here we consider the case where there are only
405 two phenotypes (A and a) and the heterozygous phenotype is A with probability h and a with
406 probability $1 - h$. In this case, the mating probability between heterozygote (Aa × Aa) is

407
$$\left[h^2 + (1-h)^2 + 2h(1-h)(1-r)\right]y^2 = \left[1 - 2h(1-h)r\right]y^2. \qquad \text{(H1)}$$

408 Therefore the frequencies after mating are

$$x' = x^2 + \left[1-(1-h)r\right]xy + \frac{1}{4}\left[1-2h(1-h)r\right]y^2,$$

$$y' = \left[1-(1-h)r\right]xy + 2(1-r)xz + \frac{1}{2}\left[1-2h(1-h)r\right]y^2 + (1-hr)yz, \qquad \text{(H2)}$$

$$z' = \frac{1}{4}\left[1-2h(1-h)r\right]y^2 + (1-hr)yz + z^2,$$

where $T = 1-2r(x+hy)\left[(1-h)y+z\right]$. This is the same as (A1) when h = 0 or 1. By linearizing the dynamics (H2) after viability selection (A2) for small x and y, we have the same result as equation (3) in Appendix S1. The largest eigenvalue of the linearized system is $(1 + hs)(1 - hr)$, and the mutant can invade if and only if $(1 + hs)(1 - hr) > 1$. This condition ($s > r/(1 - hr)$) is the same as the original diploid model (Appendix S1).

For diffusion approximation analysis, we take the limit of weak fecundity and viability selections, $r \to 0$, $s \to 0$, and large population $N \to \infty$ with the products Nr and Ns being kept finite (Appendix S3). Assuming that both s and r are the order of e, a small positive constant, the change in the allele frequency p of the mutant allele A is

$$\Delta p = p(1-p)\left[-p + h(2p-1)\right]\left\{r\left[1-2p^2-4hp(1-p)\right]-s\right\} + O(\varepsilon^2). \qquad \text{(H3)}$$

Note that s in (H3) is the selection coefficient favoring the phenotype A. From (H3) we have the frequency dynamics:

$$\dot{p} = p(1-p)\left[-p + h(2p-1)\right]\left\{r\left[1-2p^2-4hp(1-p)\right]-s\right\}. \qquad \text{(H4)}$$

When h = 1/2, this is a half of the haploid model (equation 8). The dynamics has two stable equilibria at p = 0 and p = 1, and an internal unstable equilibrium at $p_c = \frac{h}{2h-1} - \frac{\sqrt{(2h^2-2h+1)r+(2h-1)s}}{\sqrt{2r}(2h-1)}$ when $r > s$. The relative fixation rate of a single mutant relative to that of a neutral mutant is given by $\phi = 2N\rho$:

$$\phi = \frac{1}{\int_0^1 \exp\left\{-\frac{y}{2}\left[y+2h(1-y)\right]\left[R(1-y)(1-2hy+y)-S\right]\right\}dy}. \qquad \text{(H5)}$$

where $R = 4Nr$ and $S = 4Ns$. As shown in Figure S3, the lowest fixation probability is obtained when h = 1/2. When h = 1/2, the fixation probability is exactly the same as the haploid model (Figs. 4G, 4H).

Exact fixation probabilities without approximation in small populations are also calculated as Appendix S6. Results are shown in Fig. 4B (the dotted dark-green line).

435 **Literature Cited**

436 Guckenheimer, J. and P. Holmes (1983) Nonlinear Oscillations, Dynamical Systems, and
437 Bifurcations of Vector Fields. Springer, New York
438 Nowak, M.A., Sasaki, A., Taylor, C., and Fudenberg, D. (2004) Emergence of cooperation
439 and evolutionary stability in finite populations. Nature 428: 646-650

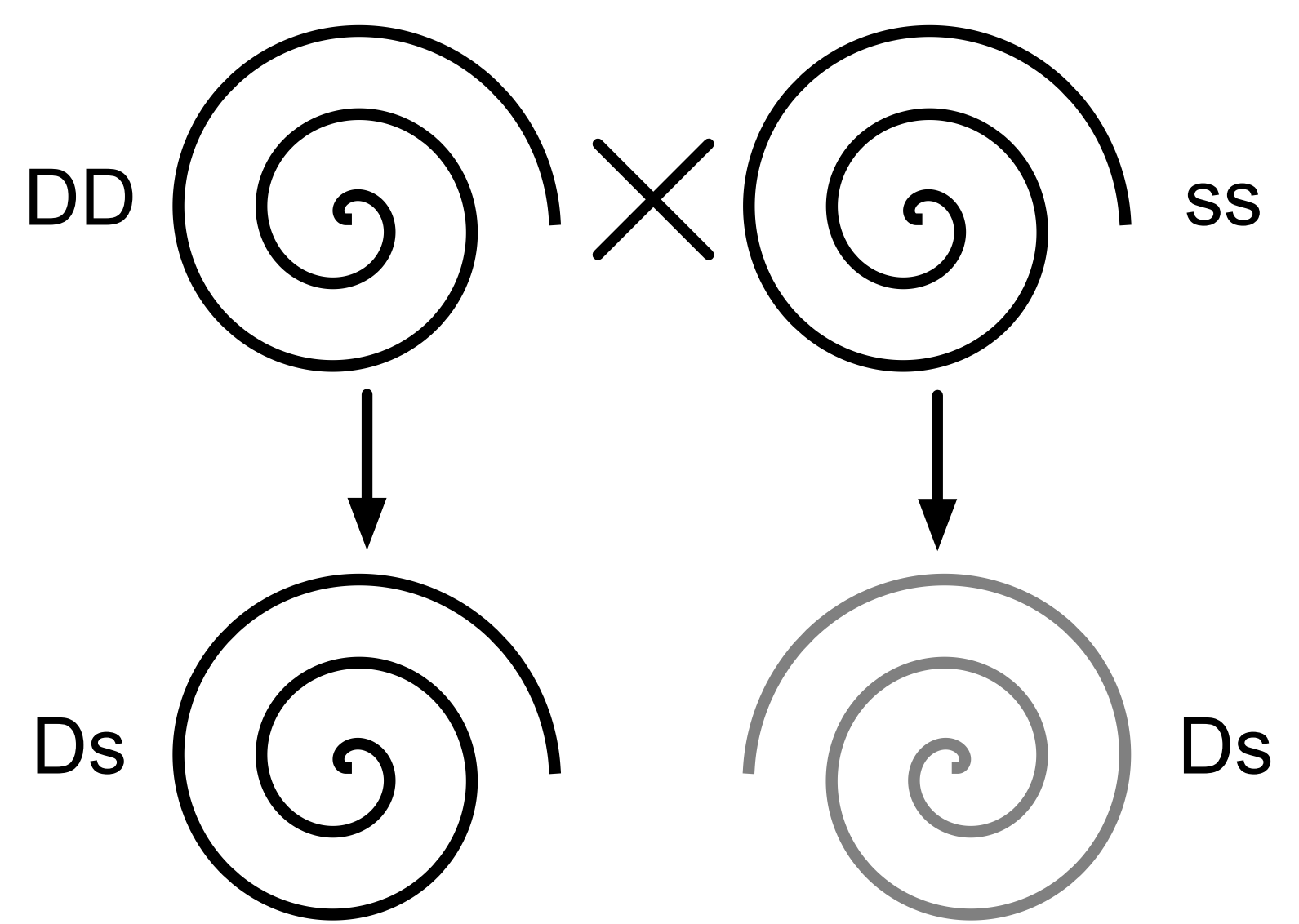
DD
ss
Ds
Ds

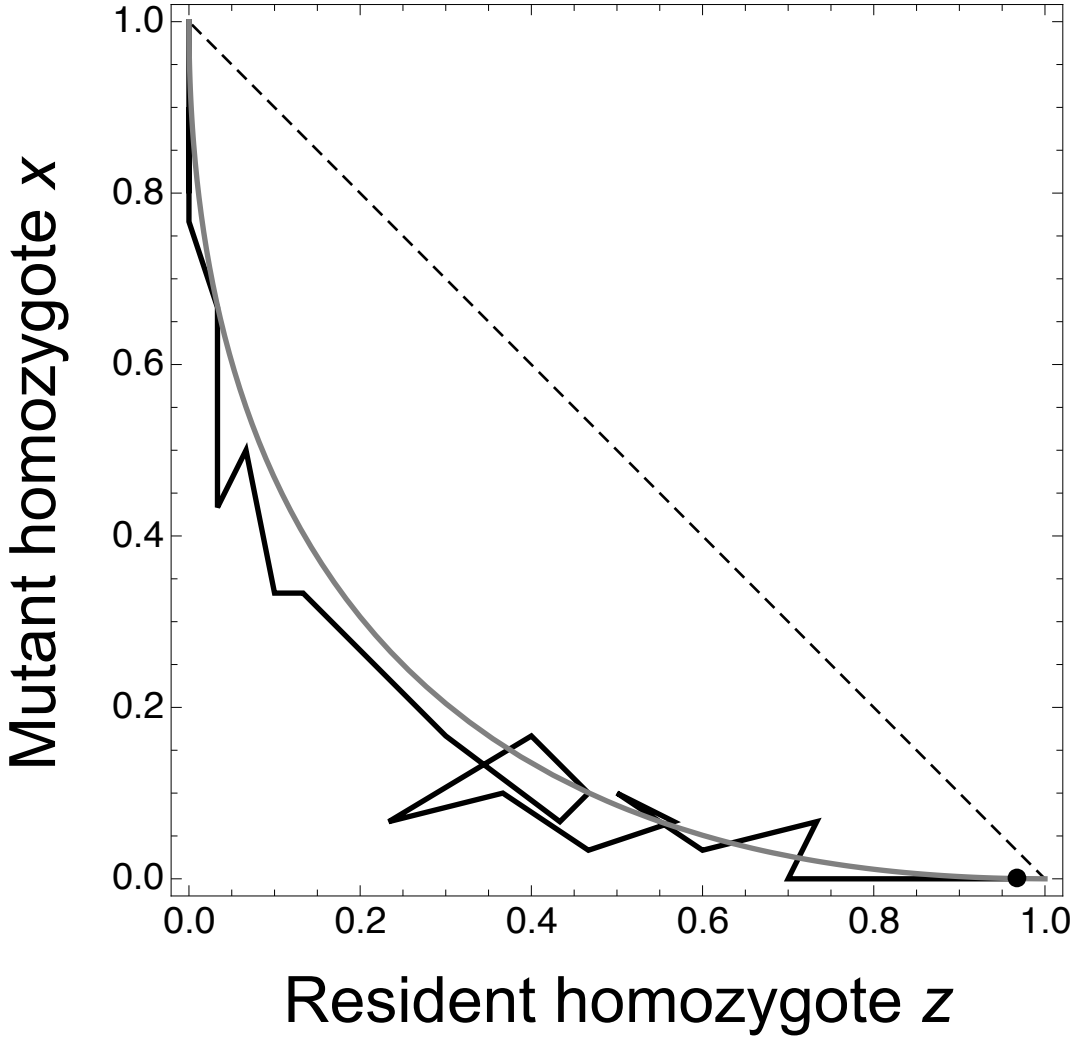
Mutant homozygote x
Resident homozygote z
0.0
0.2
0.4
0.6
0.8
1.0

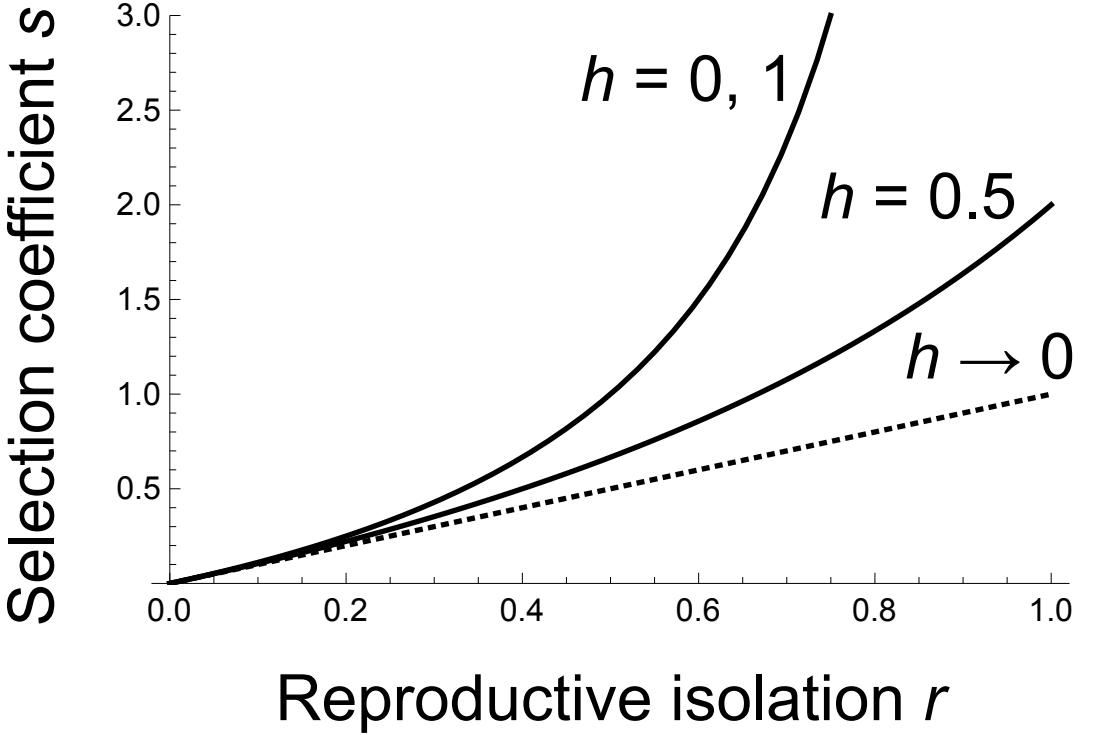
Selection coefficient s
3.0
2.5
2.0
1.5
1.0
0.5
0.0
0.2
0.4
0.6
0.8
1.0
h = 0, 1
h = 0.5
h → 0
Reproductive isolation r

A

B

C

D

Scaled derivative $\frac{1}{r}\frac{dp}{dt}$

0.10
0.05
−0.05
−0.10
0.2
0.4
0.6
0.8
1.0

Haloid

Dominant mutant

Dominant mutant with DI

Recessive mutant

Recessive mutant with DI

Mutant allele frequency p

Haploid

Diploid

Diploid with delayed inheritance

N = 3 (first step analysis & simulation)

N = 10 (simulation)

N → ∞ (diffusion approximation)
N = 1000 (simulation)

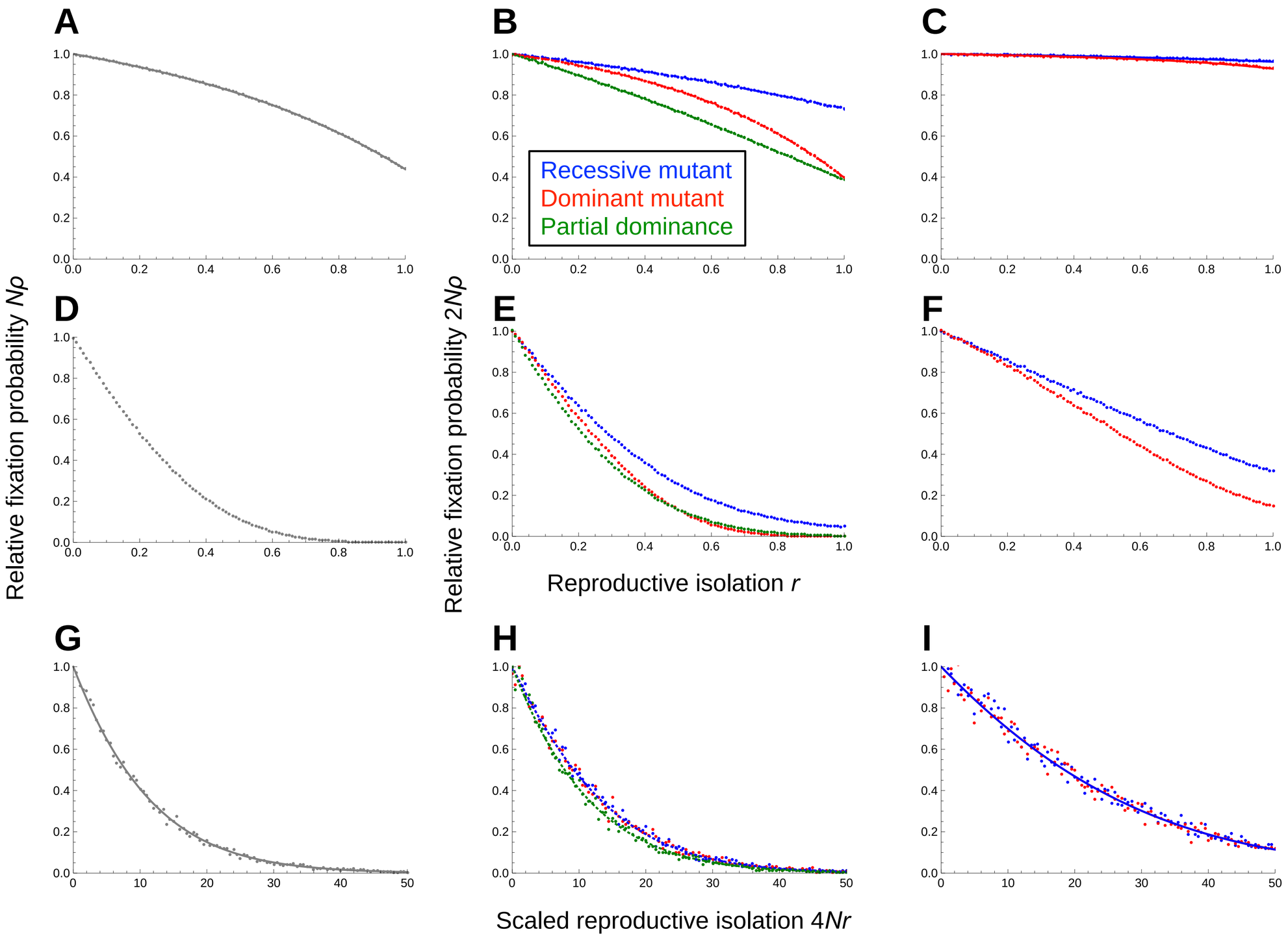

A $N = 3$ (first step analysis)

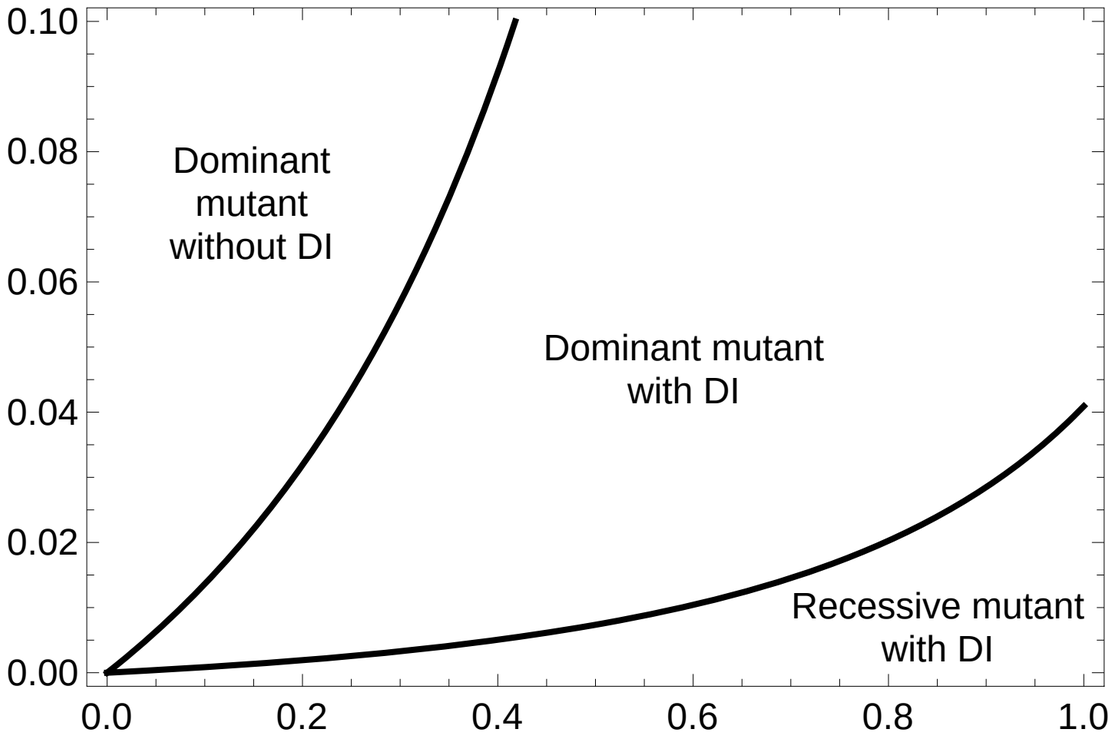

B $N = 10$ (simulation)

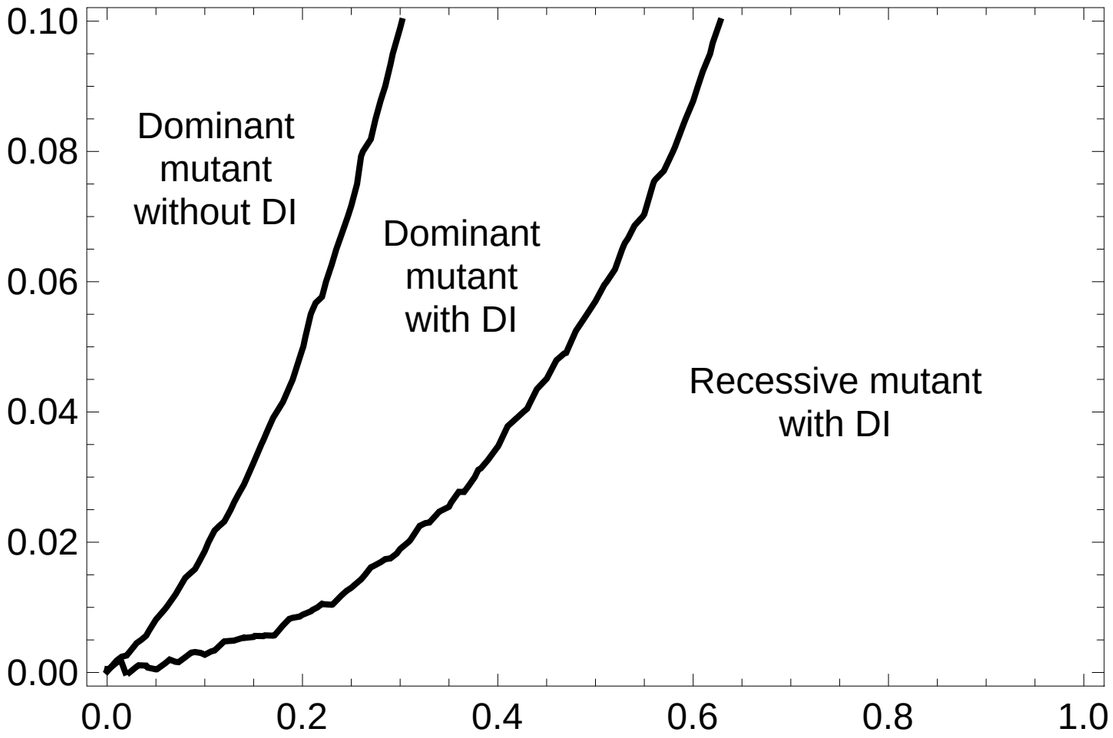

Selection coefficient s

Reproductive isolation r

C $N \rightarrow \infty$ (diffusion approximation)

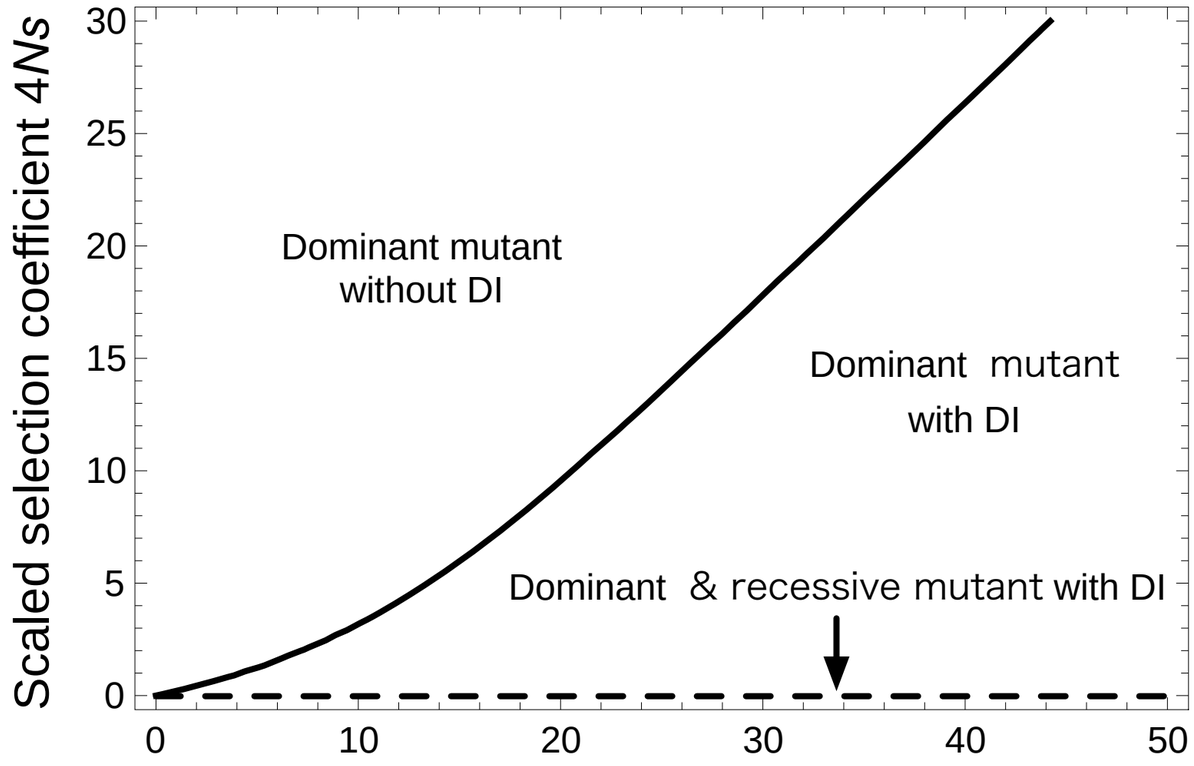

Scaled selection coefficient $4Ns$

Scaled reproductive isolation $4Nr$

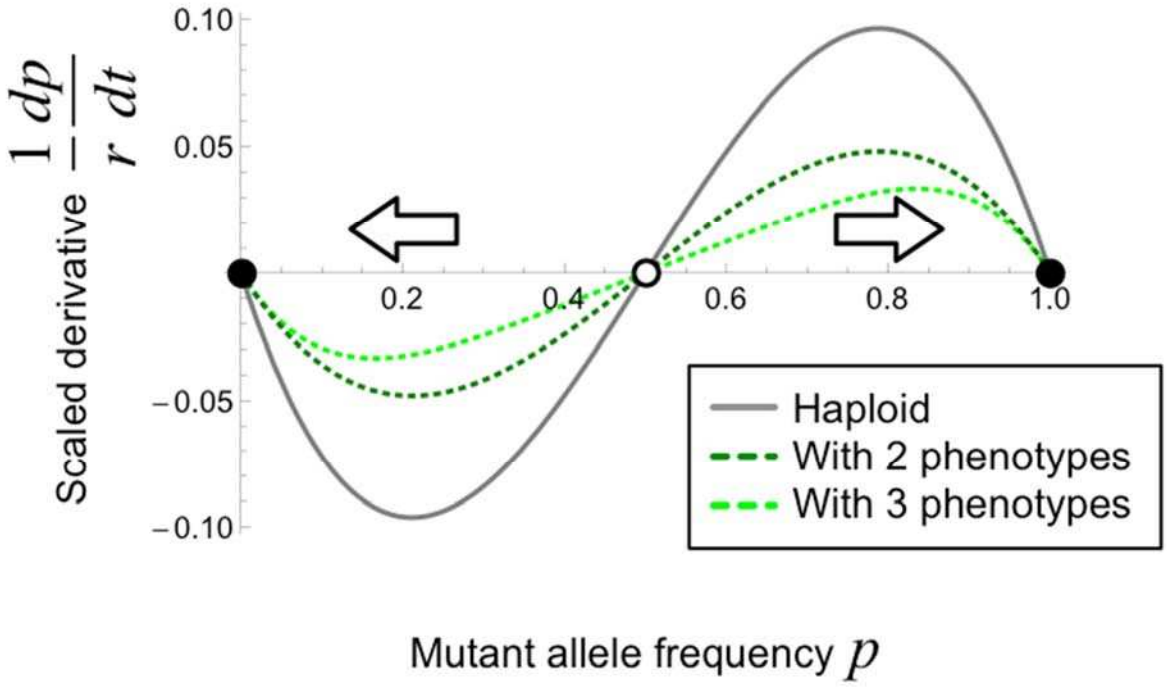

Figure S1: Allele frequency dynamics affected by positive frequency-dependent selection due to reproductive isolation (indicated by white arrows). *X*-axis: the mutant allele frequency (p). *Y*-axis: scaled derivatives of the mutant allele ($\dot{p}/r$). The haploid model (the solid gray line, eq. 8 when $s = 0$), the partial dominance model with two phenotypes (the dotted dark-green line, eq. H5 when $s = 0$ and $h = 1/2$), and the partial dominance model with three phenotypes (the dotted lime-green line, eq. 10 when $s = 0$ and $h = 1/2$). An unstable equilibrium at $p = 1/2$ (the white point) divides two basins of attraction. Stable equilibria are at $p = 0$ and 1 (the black points).

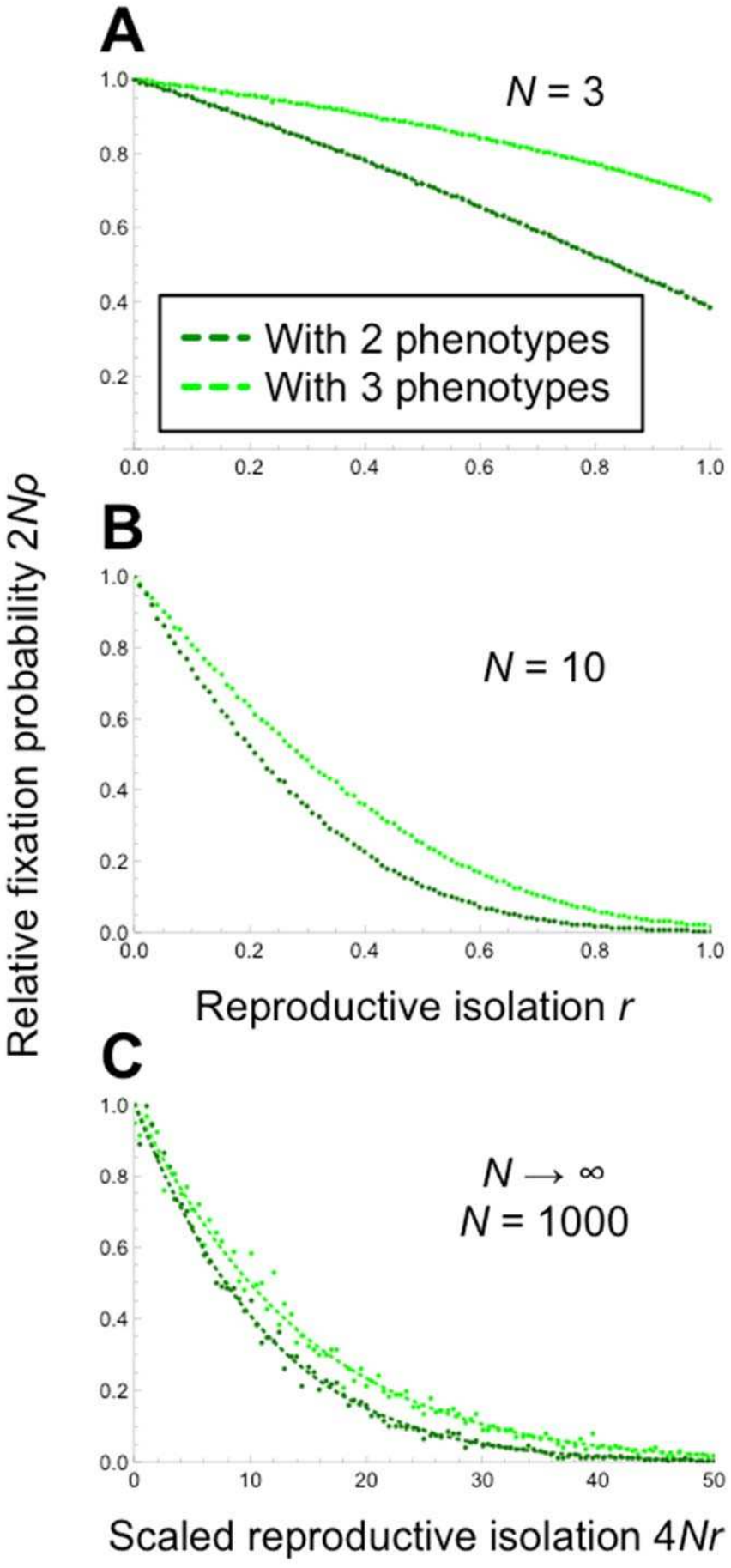
A
N = 3
With 2 phenotypes
With 3 phenotypes
B
N = 10
Reproductive isolation r
C
N → ∞
N = 1000
Relative fixation probability 2Nρ
Scaled reproductive isolation 4Nr

Figure S2: Relative fixation probabilities of a single mutant with reproductive isolation (and without viability selection: $s = 0$) to that of a neutral mutant. A, B: X-axis is the reproductive isolation parameter (r). C: X-axis is four times the product of the reproductive isolation parameter and the effective population size ($4Nr$). Y-axis is the product of fixation probability and effective population size ($2N\rho$). A: $N = 3$ (the first step analysis and Monte Carlo simulations), C: $N = 10$ (Monte Carlo simulations), C: $N \rightarrow \infty$ (diffusion approximation) and $N = 1000$ (Monte Carlo simulations). Dotted dark-green lines: the partial dominance model with two phenotypes. Dotted lime-green lines: the partial dominance model with three phenotypes.

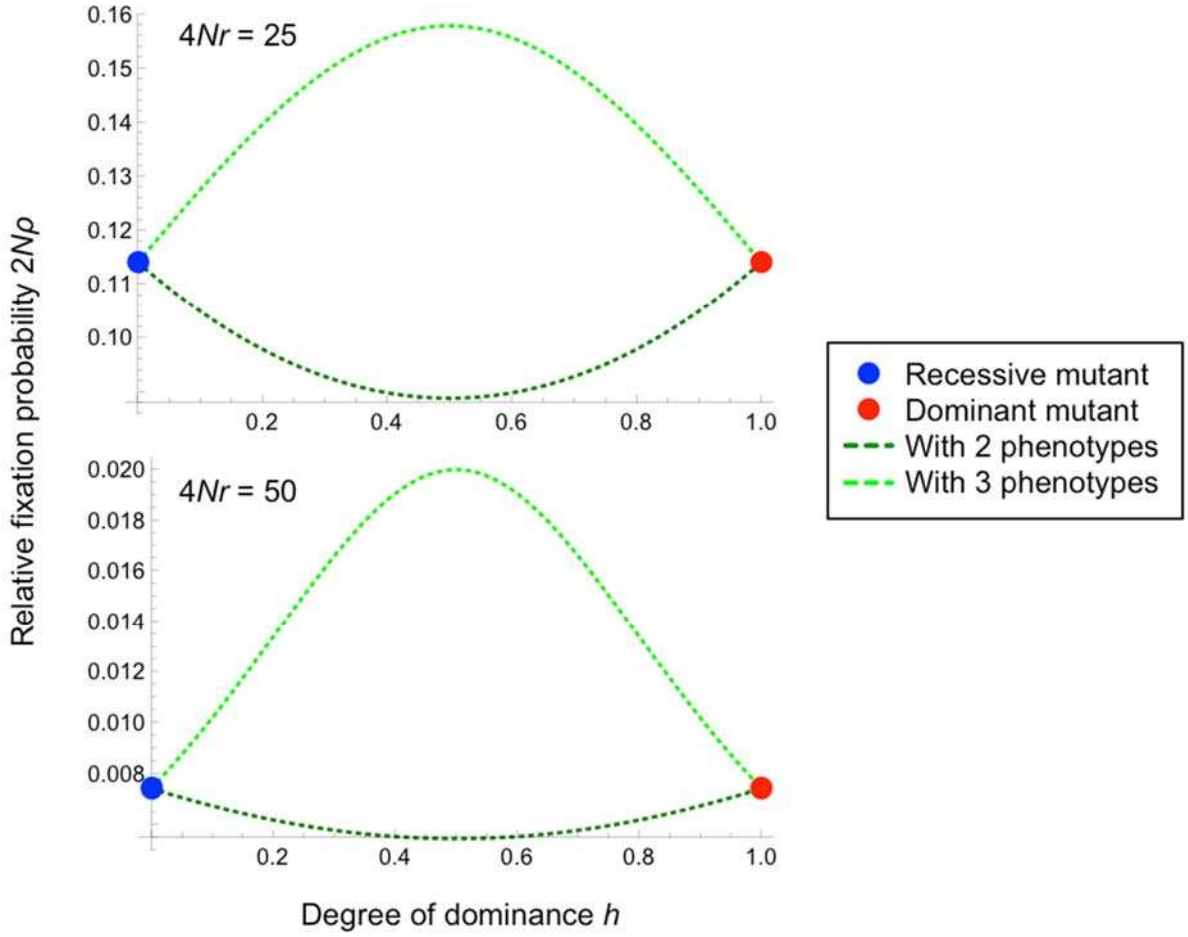

Figure S3: Effects of partial dominance in the diploid model without delayed inheritance in large populations. Blue points: the recessive mutant (h = 0). Red points: the dominant mutant (h = 1). Dotted dark-green lines: the partial dominance model with two phenotypes. Dotted lime-green lines: the partial dominance model with three phenotypes. When R (= $4Nr$) = 0, the fixation probability is 1 regardless of h values.

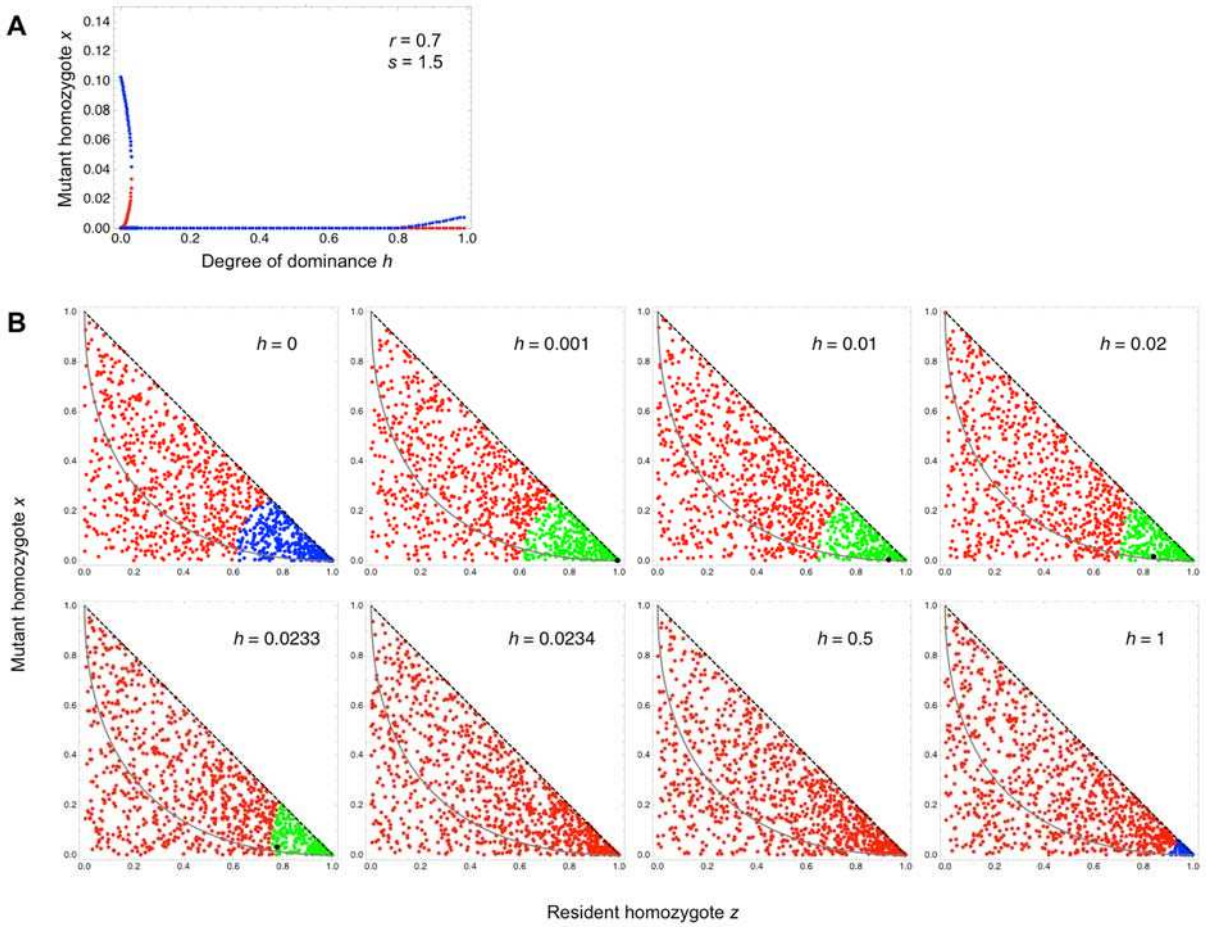

Figure S4: A: The bifurcation plot along the degree of dominance parameter (h). Y-axis is the frequency of the mutant homozygote (x). Red points: stable equilibria. Blue points: unstable equilibria. B: Simulation results of deterministic recursion equations (3)-(4). Red points: basin of attraction toward a stable equilibrium of the mutant allele. Blue points: basin of attraction toward a stable equilibrium of the resident allele. Green points: basin of attraction toward a stable equilibrium of both the mutant and resident alleles. The coexistence equilibria are shown as black points. The parameter condition is $r = 0.7$ and $s = 1.5$.

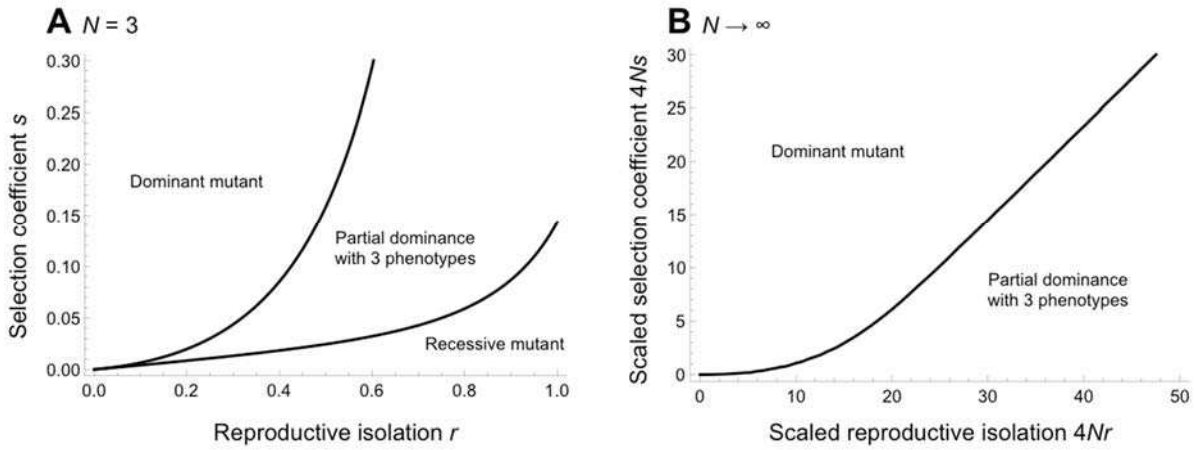

Figure S5: The alleles with the highest fixation probabilities in the diploid model without delayed inheritance given certain strength of reproductive isolation and viability selection. A: $N = 3$ (the first step analysis), B: $N \rightarrow \infty$ (diffusion approximation).

Table S1: The diploid model with delayed inheritance (when A is a dominant allele)

Mating comb.	Mating probability	AA_A	Aa_A	Aa_a	aa_A	aa_a
$AA_A \times AA_A$	x_A^2	1	0	0	0	0
$AA_A \times Aa_A$	$2x_A y_A$	1/2	1/2	0	0	0
$AA_A \times Aa_a$	$2(1-r)x_A y_a$	1/2	1/2	0	0	0
$AA_A \times aa_A$	$2x_A z_A$	0	1/2	1/2	0	0
$AA_A \times aa_a$	$2(1-r)x_A z_a$	0	1/2	1/2	0	0
$Aa_A \times Aa_A$	y_A^2	1/4	1/2	0	1/4	0
$Aa_A \times Aa_a$	$2(1-r)y_A y_a$	1/4	1/2	0	1/4	0
$Aa_A \times aa_A$	$2y_A z_A$	0	1/4	1/4	1/4	1/4
$Aa_A \times aa_a$	$2(1-r)y_A z_a$	0	1/4	1/4	1/4	1/4
$Aa_a \times Aa_a$	y_a^2	1/4	1/2	0	1/4	0
$Aa_a \times aa_A$	$2(1-r)y_a z_A$	0	1/4	1/4	1/4	1/4
$Aa_a \times aa_a$	$2y_a z_a$	0	1/4	1/4	1/4	1/4
$aa_A \times aa_A$	z_A^2	0	0	0	0	1
$aa_A \times aa_a$	$2(1-r)z_A z_a$	0	0	0	0	1
$aa_a \times aa_a$	z_a^2	0	0	0	0	1